CHAPTER 4

RESULTS

4.1 Diversity of cyanobacterial morphotypes

Upon microscopic observation of cyanobacterial mat samples across the range from 40 to 75°C from 6 hot springs which include San Kamphaeng, Pong Dued and Theppanom, Chiang Mai Province in northern Thailand, Pra Rueang, Kamphaeng Phet Province in central Thailand, Raksawarin Public Park, Ranong Province and Khaochaison, Phattalung Province in southern Thailand, 14 distinct morphotypic species of cyanobacteria were found to display the forms shown in Figures 6-11. These could be classified into 5 orders and 13 genera. The main characteristics of cyanobacterial morphotype are described in Table 3. The abundance of each species within each temperature range throughout all springs was assigned a numerical rank derived from the abundance data. The mat samples from Pong Dued (PD) Hot Spring showed the most diverse cyanobacterial morphotype assemblages, 14 morphotypic species followed by those of Theppanom (TP), 12 morphotypic species; San Kamphaeng (SK), 11 morphotypic species; Raksawarin Public Park (RS), 7 morphotypic species; Khaochaison (KC) and Pra Rueang (PR), 5 morphotypic species; in that order (Tables 4-9).

The most abundant forms in all northern hot springs (SK, PD and TP) were *Cyanothece* sp. (Figures 6C, 7C) and *Synechococcus* cf. *lividus* Copeland (Figures 6D, 7D), which dominated the 60–75°C range, and formed a thin brown, green or yellow-green mat on the surface of the flowing hot spring waters. *Phormidium* cf. *boryanum* (Bory ex Gomont) Anagnostidis and Komárek (Figures 8F, 9E), which occurred in all temperature intervals up to 60°C and dominated the 45–50°C, 50–55 and 55-60°C ranges in Pong Deud, San Kamphaeng and Theppanom Hot Springs, formed a dull green mat on the top of the surface (Sompong *et al*., 2005). *Phormidium* cf. *boryanum* was not found in any of the hot springs outside of the Chiang Mai region.

The most abundant forms in all southern hot springs (RS and KC) were *Leptolyngbya* sp. (Figures 8B, 9B) and *Mastigocladus* cf. *laminosus* Cohn (Figures 10B, 11B), which dominated the 40-60°C range. *Leptolyngbya* sp. formed a soft green, blue-green mat, but *Mastigocladus* cf. *laminosus* formed a spongy green or yellow-green mat. In central hot spring (PR), the most abundant form in this hot spring was *Phormidium* sp. (Figures 8E, 9F), which dominated in the lower temperature (40-50°C) range, and formed a firmly thin brown, green or yellow-green mat on the surface of the flowing hot spring waters.

Twelve taxa were restricted to the temperature range below 60°C, while six of these were restricted to temperatures below 50°C where *Scytonema* cf. *coactile* Montagne (Figures 10C, 11C) and *Calothrix* cf. *thermalis* (Schwabe) Hansgirg (Figures 10A, 11A) dominated. Species of these two genera have the lowest thermal tolerance (Sompong *et al*., 2005). In addition, there was a geographic distribution of thermophilic cyanobacteria with only four species [*Cyanosarcina* sp. (Figures 6B, 7B), *Chroococcidiopsis* sp. (Figures 6E, 7E), *Synechococcus* cf. *lividus* (Figures 6D, 7D) and *Leptolyngbya* sp. (Figures 8B, 9B)] occurring in all six hot springs.

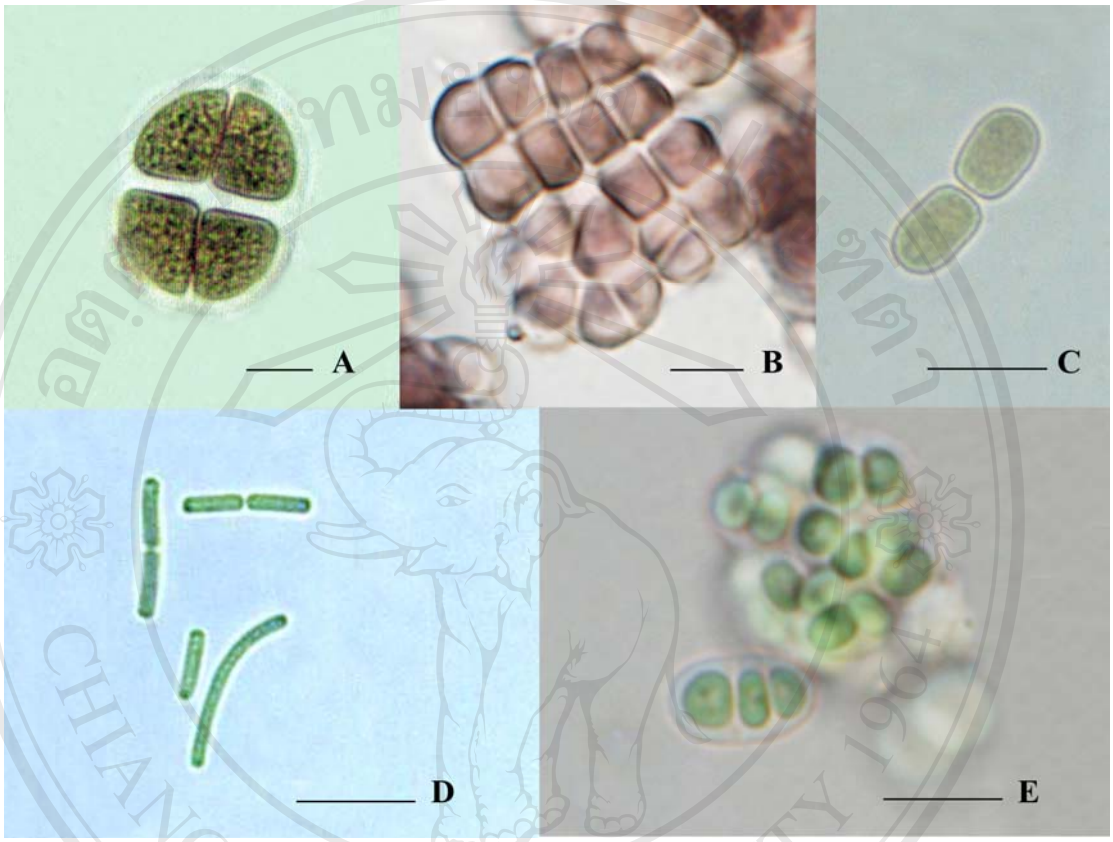

(scale bar: 10 μm)

Figure 6. Cyanobacterial morphotypes in Orders Chroococcales and Pleurocapsales from natural samples in six hot springs of Thailand

(A-D) Chroococcales; (A) *Chroococcus* sp., (B) *Cyanosarcina* sp., (C) *Cyanothece* sp., (D) *Synechococcus* cf. *lividus* Copeland, (E) Pleurocapsales; *Chroococcidiopsis* sp.

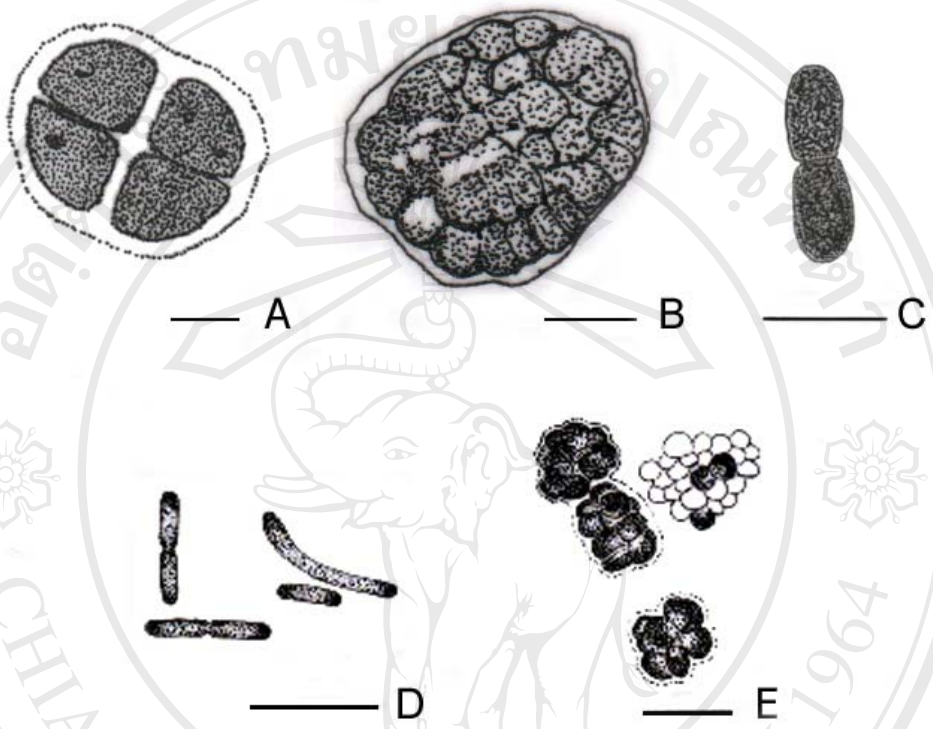

(scale bar: 10 μm)

Figure 7. Hand-drawings of cyanobacterial morphotypes in Orders Chroococcales and Pleurocapsales from natural samples in six hot springs of Thailand

(A-D) Chroococcales; (A) *Chroococcus* sp., (B) *Cyanosarcina* sp., (C) *Cyanothece* sp., (D) *Synechococcus* cf. *lividus* Copeland, (E) Pleurocapsales; *Chroococcidiopsis* sp.

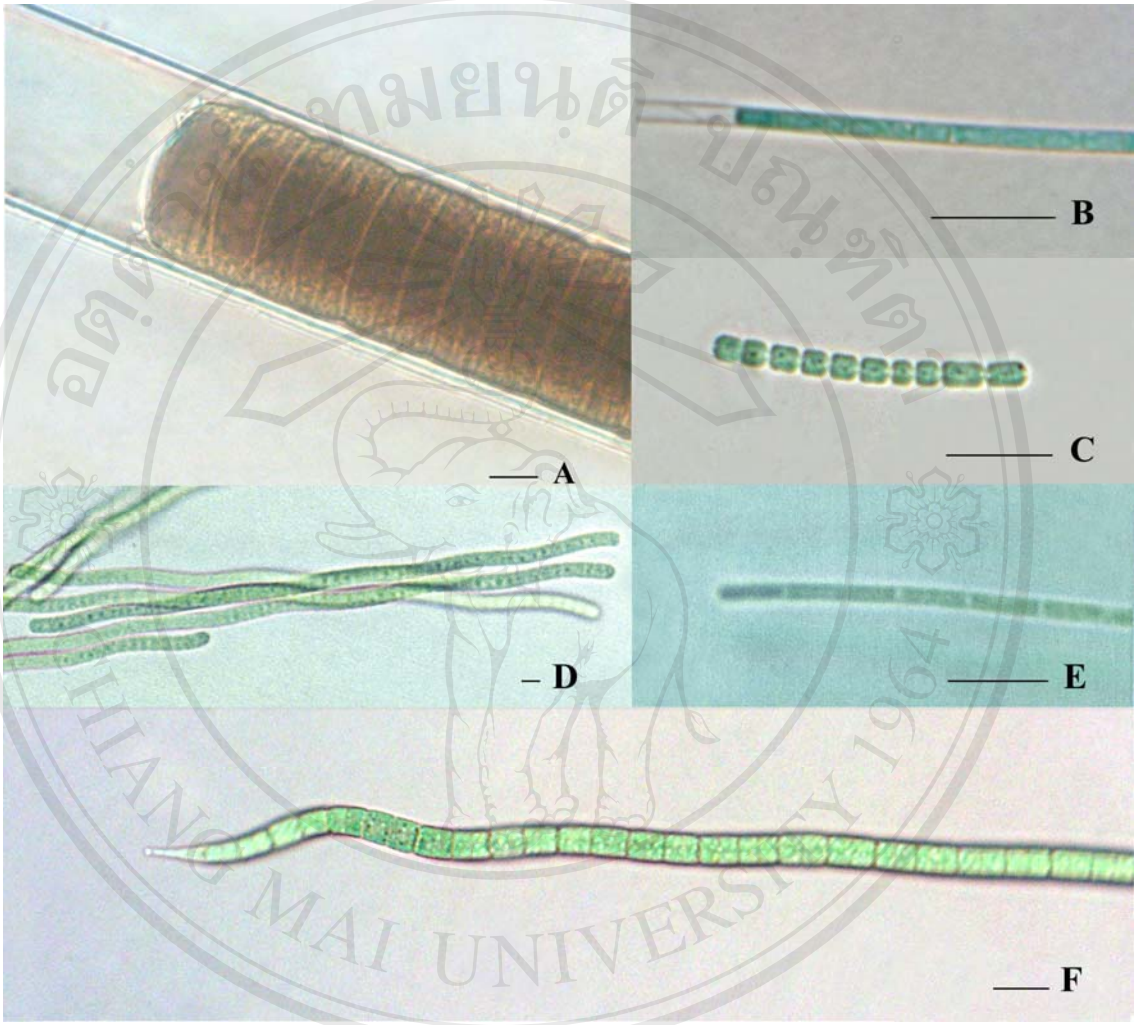

(scale bar: 10 μm)

Figure 8. Cyanobacterial morphotypes in Order Oscillatoriales from natural samples in six hot springs of Thailand

(A) *Lyngbya* sp., (B) *Leptolyngbya* sp., (C) *Pseudanabaena* sp., (D) *Oscillatoria* sp., (E) *Phormidium* sp., (F) *Phormidium* cf. *boryanum* (Bory ex Gomont) Anagnostidis and Komárek

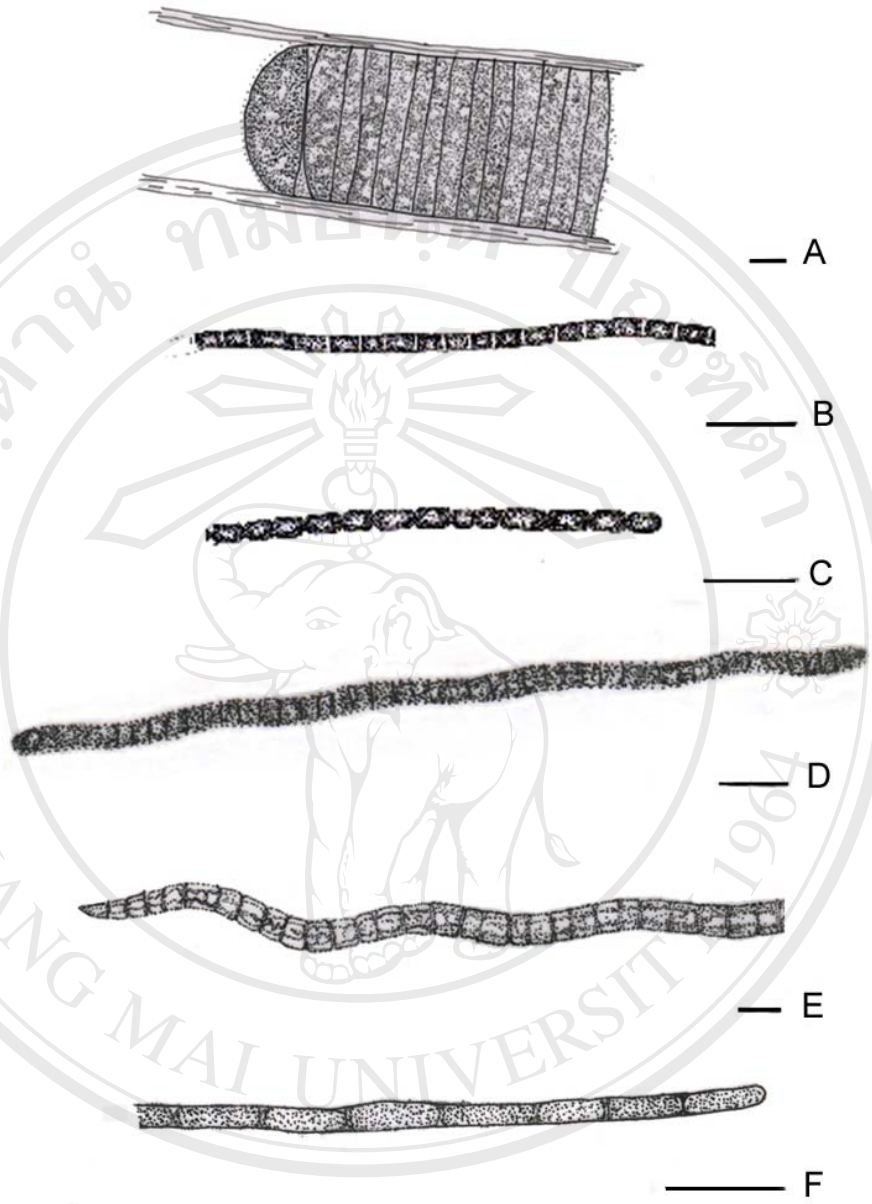

(scale bar: 10 μm)

Figure 9. Hand-drawings of cyanobacterial morphotypes in Order Oscillatoriales from natural samples in six hot springs of Thailand

(A) *Lyngbya* sp., (B) *Leptolyngbya* sp., (C) *Pseudanabaena* sp., (D) *Oscillatoria* sp., (E) *Phormidium* cf. *boryanum* (Bory ex Gomont) Anagnostidis and Komárek, (F) *Phormidium* sp.

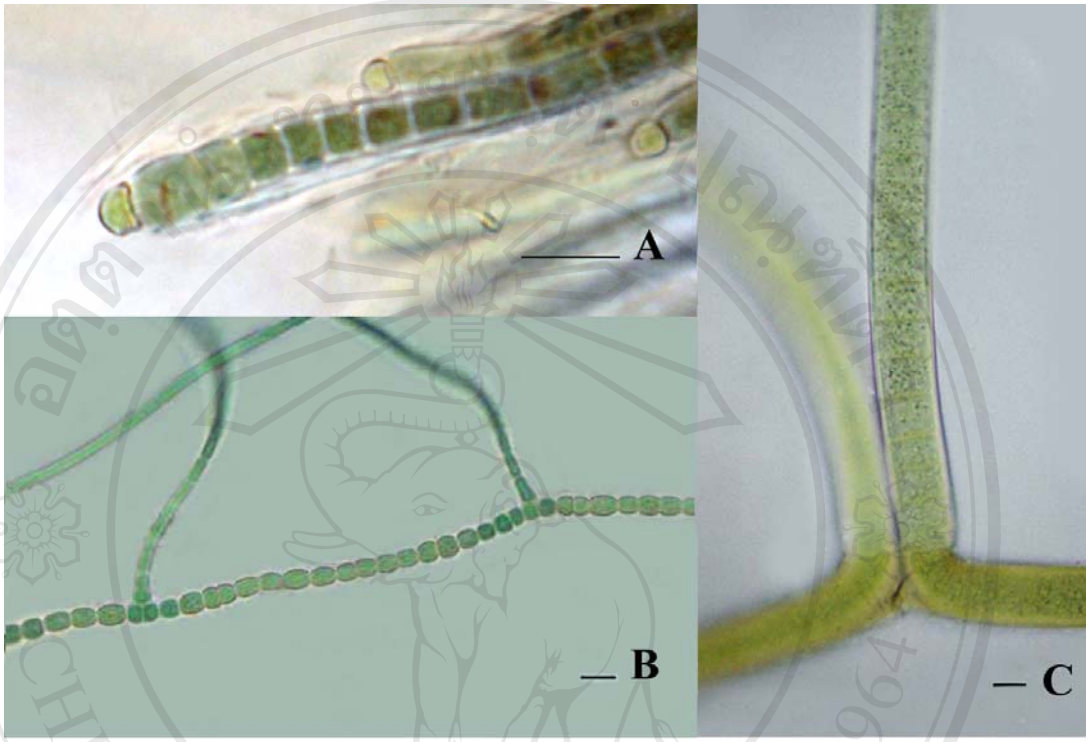

(scale bar: 10 μm)

Figure 10. Cyanobacterial morphotypes in Order Nostocales and Stigonematales from natural samples in six hot springs of Thailand

(A) Nostocales; *Calothrix* cf. *thermalis* (Schwabe) Hansgirg, (B) Stigonematales; *Mastigocladus* cf. *laminosus* Cohn, (C) Nostocales; *Scytonema* cf. *coactile* Montagne

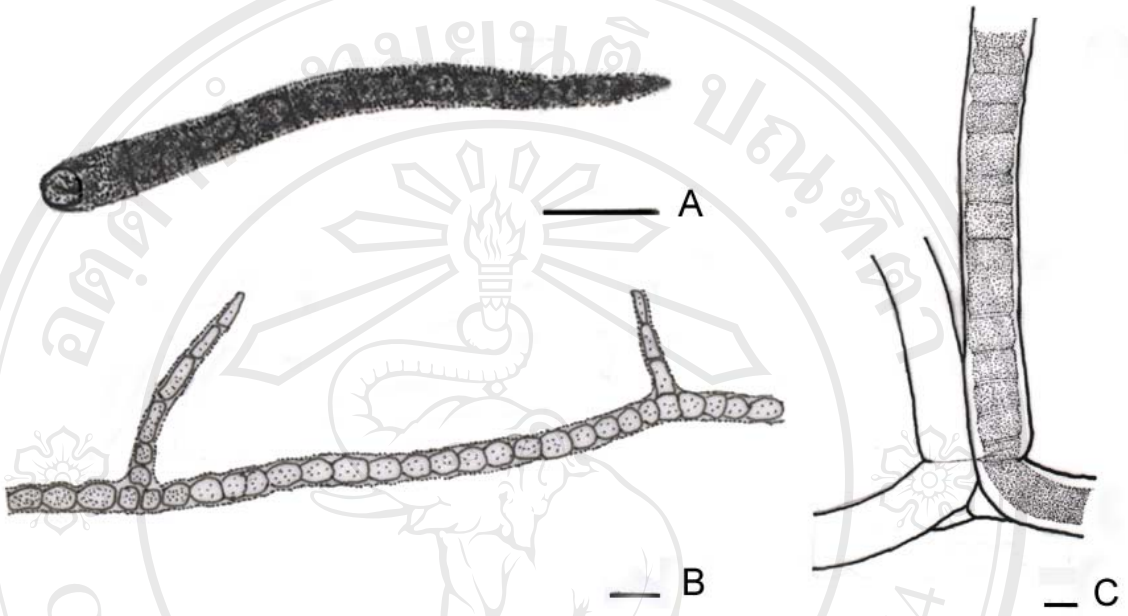

(scale bar: 10 μm)

Figure 11. Hand-drawings of cyanobacterial morphotypes in Order Nostocales and Stigonematales from natural samples in six hot springs of Thailand

(A) Nostocales; (A) *Calothrix* cf. *thermalis* (Schwabe) Hansgirg, (B) Stigonematales; *Mastigocladus* cf. *laminosus* Cohn, (C) Nostocales; *Scytonema* cf. *coactile* Montagne

Table 3. Cyanobacterial morphotypes distinguished in six hot springs

Morphotypes (main characteristics)	Assignment species
Order Chroococcales	
Cells colonial, mucilaginous envelopes colorless. Cells spherical or hemispherical, pale or dull blue-green, without a sheath 8-15 μm diameter.	*Chroococcus* sp.
Cells colonial, subspherical-irregular colonies, more or less with densely aggregated cells, with or without mucilaginous envelopes, blue-green, 4-6 μm diameter.	*Cyanosarcina* sp.
Cells solitary, rod-shaped or hemi-cylindrical, straight with rounded ends, thalli thin, brownish or dull blue-green, 8–10 × 5–7 μm.	*Cyanothece* sp.
Cells solitary, rod-shaped, straight or slightly curved, with rounded ends, pale blue-green or blue-green, 5–15 × 1.5–2.5 μm.	*Synechococcus* cf. *lividus* Copeland
Order Pleurocapsales	
Cells solitary, spherical, or in colonies usually of varied size, spherical or irregular colonies surrounded by thin mucilaginous envelopes (sheaths). Some cells later change into baeocytes, blue-green; 1.5-2.0 μm diameter.	*Chroococcidiopsis* sp.

Table 3. (continue)

Morphotypes (main characteristics)	Assignment species
Order Oscillatoriales	
Filamentous form without heterocysts or akinetes, straight, forming into fasciculate thallus, brownish black or brownish green. Trichome cylindrical, unbranched, distinct and persistent sheath, sheath thick, only one trichome in a sheath, unconstricted at the cross walls, 25–35 μm broad, 3–4 μm long.	*Lyngbya* sp.
Filamentous form without heterocysts or akinetes, straight, forming into thallus, green or blue-green, trichome cylindrical, unbranched, sheaths thin, only one trichome in a sheath, unconstricted at the cross walls, 1.5–2.0 μm broad, 2.0 μm long.	*Leptolyngbya* sp.
Filamentous form without heterocysts or akinetes, straight, forming into thallus, green or blue-green, trichome cylindrical, unbranched, unconstricted at the cross walls, 3-4 μm broad, 4-5 μm long.	*Oscillatoria* sp.
Filamentous form without heterocysts or akinetes, trichomes forming into thalli, thalli expanded, more or less thin. Trichomes spiral, fully coiled or only at the apices, slightly constricted at the cross walls, sheaths firm, trichomes clearly motile (gliding or waving), blackish blue-green or blue-green, cells 7-10 μm broad, 3-5 μm long.	*Phormidium* cf. *boryanum* (Bory ex Gomont) Anagnostidis and Komarek
Filamentous form without heterocysts or akinetes, straight, forming into thallus, blue-green, trichome cylindrical, unbranched, unconstricted at the cross walls, 2.5-3 μm broad, 5-7 μm long.	*Phormidium* sp.

Table 3. (continue)

Morphotypes (main characteristics)	Assignment species
Order Oscillatoriales (continue)	
Filamentous form without heterocysts or akinetes, trichomes solitary or in fine mats, cells cylindrical, both ends truncated, terminal aerotopes forming at both ends, firm sheaths lacking, trichomes without any branching, cross walls slightly constricted, 3-5 μm broad, 4-5 μm wide.	*Pseudanabaena* sp.

Table 3. (continue)

Morphotypes (main characteristics)	Assignment species
Order Nostocales	
Filamentous form with heterocysts or akinetes, heterocysts basal, ellipsoidal to subspherical, thallus expanded, mucilaginous, blue-green or brownish-green. Filaments single or in small bundles, unbranched, flexuous, cells 6-7 × 4-5 μm at the base; cells 2 × 2-3 μm.	*Calothrix* cf. *thermalis* (Schwabe) Hansgirg
Filamentous form with heterocysts and/or akinetes, heterocysts sparse, falsely branched, trichomes solitary in each sheath, straight, forming thalli, thalli expanded, woolly, brownish-black or brown, filament 16-24 μm broad, false branches long, erect, trichomes 12-20 μm broad.	*Scytonema* cf. *coactile* Montagne
Order Stigonematales	
Filamentous form with heterocysts and/or akinetes, trichomes with reversed 'V'-shaped branching; true branching present, heterocysts intercalary, spherical or barrel-shaped, green or blue-green, 4-8 μm broad, side branches about 3 μm broad.	*Mastigocladus* cf. *laminosus* Cohn

Table 4. Abundance of cyanobacterial morphotypes at San Kamphaeng (SK) Hot Spring in every season and for each range of temperature

Cyanobacterial morphotypes	Abundance[a] in																	
	40-45°C			45-50°C			50-55°C			55-60°C			60-65°C			65-70°C		
	Rainy	Cold dry	Summer	Rainy	Cold dry	Summer	Rainy	Cold dry	Summer	Rainy	Cold dry	Summer	Rainy	Cold dry	Summer	Rainy	Cold dry	Summer
	SK40-r	SK40-w	SK40-s	SK45-r	SK45-w	SK45-s	SK50-r	SK50-w	SK50-s	SK55-r	SK55-w	SK55-s	SK60-r	SK60-w	SK60-s	SK65-r	SK65-w	SK65-s
Chroococcales																		
Chroococcus sp.	-	+	+	-	-	-	-	-	-	-	-	-	-	-	-	-	-	-
Cyanosarcina sp.	+	+	+	-	-	-	-	-	-	-	-	-	-	-	-	-	-	-
Cyanothece sp.	-	-	-	-	+	+	+	-	++	+++	+++	+++	+++	+++	+++	+++	+++	+++
Synechococcus cf. *lividus* Copeland	-	-	+	+	+	+	++	+++	+++	+++	++	++	++	++	++	+	+	+
Pleurocapsales																		
Chroococcidiopsis sp.	++	++	++	-	+	+	-	-	-	-	-	-	-	-	-	-	-	-
Oscillatoriales																		
Leptolyngbya sp.	+	+	-	-	-	-	-	-	-	-	-	-	-	-	-	-	-	-
Oscillatoria sp.	+	+	++	-	-	-	-	-	-	-	-	-	-	-	-	-	-	-
Phormidium cf. *boryanum* (Bory ex Gom.)Anagn. et Kom.	+++	+++	+++	+++	+++	+++	+++	+++	+++	+++	+++	++	-	-	-	-	-	-
Phormidium sp.	-	+	+	-	-	-	-	-	-	-	-	-	-	-	-	-	-	-
Pseudanabaena	-	+	+	-	-	-	-	-	-	-	-	-	-	-	-	-	-	-
Stigonematales *Mastigocladus* cf. *laminosus* Cohn	+	-	+	-	-	-	-	-	-	-	-	-	-	-	-	-	-	-

[a] +++ = dominant >30% of the population; ++ = common 1–30%; + = rare <1%; - = not detected

Table 5. Abundance of cyanobacterial morphotypes at Pong Dued (PD) Hot Spring in every season and for each range of temperature

Cyanobacterial morphotypes	Abundance[a] in																				
	40-45°C			45-50°C			50-55°C			55-60°C			60-65°C			65-70°C			70-75°C		
	Rainy	Cold dry	Summer	Rainy	Cold dry	Summer	Rainy	Cold dry	Summer	Rainy	Cold dry	Summer	Rainy	Cold dry	Summer	Rainy	Cold dry	Summer	Rainy	Cold dry	Summer
	PD40-r	PD40-w	PD40-s	PD45-r	PD45-w	PD45-s	PD50-r	PD50-w	PD50-s	PD55-r	PD55-w	PD55-s	PD60-r	PD60-w	PD60-s	PD65-r	PD65-w	PD65-s	PD70-r	PD70-w	PD70-s
Chroococcales																					
Chroococcus sp.	+	++	++	-	++	+	-	-	-	-	-	-	-	-	-	-	-	-	-	-	-
Cyanosarcina sp.	-	-	-	-	+	+	-	-	-	-	-	-	-	-	-	-	-	-	-	-	-
Synechococcus sp.	-	-	-	-	-	-	++	++	+++	+++	+++	+++	+++	+++	+++	+++	+++	+++	+++	++	++
Synechococcus cf. *lividus* Copeland	-	-	-	+	+	+	++	++	+++	+++	++	++	+++	+++	+++	++	++	++	+	+	+
Pleurocapsales																					
Chroococcidiopsis sp.	++	++	++	++	++	++	++	+	-	-	-	+	-	-	+	-	-	-	-	-	-
Lyngbya sp.	+++	+++	+++	++	++	++	-	-	-	-	-	-	-	-	-	-	-	-	-	-	-
Leptolyngbya sp.	+	+	+	+	-	-	-	-	-	-	-	-	-	-	-	-	-	-	-	-	-
Oscillatoria sp.	-	-	-	-	-	-	-	-	-	-	-	-	-	-	-	-	-	-	-	-	-
Phormidium cf. *boryanum* (Bory ex Gom.)Anagn. et Kom.	-	-	-	+	++	++	+++	+++	+++	+++	+++	+++	-	-	-	-	-	-	-	-	-
Phormidium sp.	-	+	-	-	-	-	+	+	+	+	-	+	-	-	-	-	-	-	-	-	-
Pseudanabaena sp.	+	++	++	-	-	+	-	-	-	-	-	-	-	-	-	-	-	-	-	-	-

[a] +++ = dominant >30% of the population; ++ = common 1–30%; + = rare <1%; - = not detected

Table 5. (continue)

Cyanobacterial morphotypes	Abundance[a] in																				
	40-45°C			45-50°C			50-55°C			55-60°C			60-65°C			65-70°C			70-75°C		
	Rainy	Cold dry	Summer	Rainy	Cold dry	Summer	Rainy	Cold dry	Summer	Rainy	Cold dry	Summer	Rainy	Cold dry	Summer	Rainy	Cold dry	Summer	Rainy	Cold dry	Summer
	PD40-r	PD40-w	PD40-s	PD45-r	PD45-w	PD45-s	PD50-r	PD50-w	PD50-s	PD55-r	PD55-w	PD55-s	PD60-r	PD60-w	PD60-s	PD65-r	PD65-w	PD65-s	PD70-r	PD70-w	PD70-s
Nostocales																					
Calothrix cf. *thermalis* (Schwabe) Hansg.	+++	+++	+++	+++	+++	+++	-	-	-	-	-	-	-	-	-	-	-	-	-	-	-
Scytonema cf. *coactile* Montagne	++	++	++	-	-	-	-	-	-	-	-	-	-	-	-	-	-	-	-	-	-
Stigonematales																					
Mastigocladus cf. *laminosus* Cohn	-	-	-	-	+	-	-	-	-	-	-	-	-	-	-	-	-	-	-	-	-

[a] +++ = dominant >30% of the population; ++ = common 1–30%; + = rare <1%; - = not detected

Table 6. Abundance of cyanobacterial morphotypes at Theppanom (TP) Hot Spring in every season and for each range of temperature

Cyanobacterial morphotypes	Abundance[a] in																				
	40-45°C			45-50°C			50-55°C			55-60°C			60-65°C			65-70°C			70-75°C		
	Rainy	Cold dry	Summer	Rainy	Cold dry	Summer	Rainy	Cold dry	Summer	Rainy	Cold dry	Summer	Rainy	Cold dry	Summer	Rainy	Cold dry	Summer	Rainy	Cold dry	Summer
	TP40-r	TP40-w	TP40-s	TP45-r	TP45-w	TP45-s	TP50-r	TP50-w	TP50-s	TP55-r	TP55-w	TP55-s	TP60-r	TP60-w	TP60-s	TP65-r	TP65-w	TP65-s	TP70-r	TP70-w	TP70-s
Chroococcales																					
Chroococcus sp.	+	+	-	-	-	-	-	-	-	-	-	-	-	-	-	-	-	-	-	-	-
Cyanosarcina sp.	+	+	+	-	-	-	-	-	-	-	-	-	-	-	-	-	-	-	-	-	-
Synechococcus sp.	-	-	-	-	-	-	+	+	+	+++	+++	+++	+++	+++	+++	+++	+++	+++	+++	+++	+++
Synechococcus cf. *lividus* Copeland	-	-	-	+	+	+	++	++	++	+++	++	++	+++	+++	+++	+++	++	++	+	+	+
Pleurocapsales																					
Chroococcidiopsis sp.	++	++	+	+	+	+	+	+	++	-	-	-	-	-	-	-	-	-	-	-	-
Lyngbya sp.	+	-	-	-	-	-	-	-	-	-	-	-	-	-	-	-	-	-	-	-	-
Leptolyngbya sp.	+	+	+	+	+	+	-	-	-	-	-	-	-	-	-	-	-	-	-	-	-
Phormidium cf. *boryanum* (Bory ex Gom.)Anagn. et Kom.	-	-	-	+++	+++	+++	+++	+++	+++	+++	+++	+++	-	-	-	-	-	-	-	-	-
Phormidium sp.	-	-	-	+	+	+	+	+	+	+	+	+	-	-	-	-	-	-	-	-	-
Pseudanabaena sp.	-	-	-	-	+	++	+	+	++	-	-	-	-	-	-	-	-	-	-	-	-

[a] +++ = dominant >30% of the population; ++ = common 1–30%; + = rare <1%; - = not detected

Table 6. (continue)

Cyanobacterial morphotypes	Abundance[a] in																				
	40-45°C			45-50°C			50-55°C			55-60°C			60-65°C			65-70°C			70-75°C		
	Rainy	Cold dry	Summer	Rainy	Cold dry	Summer	Rainy	Cold dry	Summer	Rainy	Cold dry	Summer	Rainy	Cold dry	Summer	Rainy	Cold dry	Summer	Rainy	Cold dry	Summer
	TP40-r	TP40-w	TP40-s	TP45-r	TP45-w	TP45-s	TP50-r	TP50-w	TP50-s	TP55-r	TP55-w	TP55-s	TP60-r	TP60-w	TP60-s	TP65-r	TP65-w	TP65-s	TP70-r	TP70-w	TP70-s
Nostocales																					
Calothrix cf. *thermalis* (Schwabe) Hansg.	+	+	+	++	++	++	-	_	-	-	-	-	-	-	-	-	-	-	-	-	-
Scytonema cf. *coactile* Montague	++	++	++	-	-	-	-	_	-	-	-	-	-	-	-	-	-	-	-	-	-

[a] +++ = dominant >30% of the population; ++ = common 1–30%; + = rare <1%; - = not detected

Table 7. Abundance of cyanobacterial morphotypes at Pra Rueang (PR) Hot Spring in every season and for each range of temperature

Cyanobacterial morphotypes	**Abundance[a] in**					
	40-45°C			**45-50°C**		
	Rainy	**Cold dry**	**Summer**	**Rainy**	**Cold dry**	**Summer**
	PR40-r	PR40-w	PR40-s	PR45-r	PR45-w	PR45-s
Chroococcales						
Cyanosarcina sp.	+	++	++	-	+	+
Synechococcus cf. *lividus* Copeland	-	-	-	++	++	++
Pleurocapsales						
Chroococcidiopsis sp.	++	++	++	++	++	++
Oscillatoriales						
Leptolyngbya sp.	+	+	+	+	++	++
Phormidium sp.	+++	+++	+++	+++	+++	+++

[a] +++ = dominant >30% of the population; ++ = common 1–30%; + = rare <1%; - = not detected

Table 8. Abundance of cyanobacterial morphotypes at Raksawarin Public Park (RS) Hot Spring in every season and for each range of temperature

Cyanobacterial morphotypes	Abundance[a] in											
	40-45°C			45-50°C			50-55°C			55-60°C		
	Rainy	Cold dry	Summer	Rainy	Cold dry	Summer	Rainy	Cold dry	Summer	Rainy	Cold dry	Summer
	RS40-r	RS40-w	RS40-s	RS45-r	RS45-w	RS45-s	RS50-r	RS50-w	RS50-s	RS55-r	RS55-w	RS55-s
Chroococcales												
Chroococcus sp.	-	-	+	-	-	-	-	-	-	-	-	-
Cyanosarcina sp.	-	-	-	-	-	-	+	-	-	-	-	-
Synechococcus cf. *lividus* Copeland	+	+	+	++	++	++	++	++	++	+++	++	++
Pleurocapsales												
Chroococcidiopsis sp.	+	+	+	+	++	++	+	++	++	-	-	-
Oscillatoriales												
Leptolyngbya sp.	+++	+++	+++	++	++	+++	+++	+++	+++	+++	+++	+++
Phormidium sp.	+++	+++	+++	++	+	+	+	+	+	+	+	+
Stigonematales												
Mastigocladus cf. *laminosus* Cohn	+++	+++	+++	+++	+++	+++	++	++	+++	++	++	++

[a] +++ = dominant >30% of the population; ++ = common 1–30%; + = rare <1%; - = not detected

Table 9. Abundance of cyanobacterial morphotypes at Khaochaison (KC) Hot Spring in every season and for each range of temperature

Cyanobacterial morphotypes	**Abundance[a] in**					
	45-50°C			**50-55°C**		
	Rainy	**Cold dry**	**Summer**	**Rainy**	**Cold dry**	**Summer**
	KC45-r	KC45-w	KC45-s	KC50-r	KC50-w	PKC50-s
Chroococcales						
Synechococcus cf. *lividus* Copeland	-	+	+	++	++	++
Pleurocapsales						
Chroococcidiopsis sp.	+	+	+	+	+	+
Oscillatoriales						
Leptolyngbya sp.	+++	+++	+++	+++	+++	+++
Phormidium sp.	-	-	-	++	++	++
Pseudanabaena sp.	+	++	++	-	-	-

[a] +++ = dominant >30% of the population; ++ = common 1–30%; + = rare <1%; - = not detected

4.2 Morphotypic diversity analysis

The cyanobacterial morphotypic results presented within all six hot springs in each temperature range and season were put into the SPSS using Windows version 11.5 to perform statistical analysis: Categorical Principal Components Analysis (CATPCA) of the relationships between cyanobacterial morphotype abundance and geographical distribution.

This ordination analysis quantified categorical variables while reducing the dimensionality of the data. Therefore, fewer components rather than a large number of variables can be interpreted. The mean abundance for each species for each temperature range and season were put into the SPSS. The output from the CATPCA is presented in ordination diagrams or two-dimensional scatterplot. The total eigenvalue of the ordination axis or dimension in CATPCA is used to show how much variance is accounted for by the axis (Shaw, 2003). Each cyanobacterial morphotype is represented by line and the hot springs in each temperature range and season are represented by squares. The position of the squares is based on cyanobacterial distribution in relation to the geographical position within many ranges of temperature and season. The origin represents the mean of the cases (all hot springs in each temperature range and season) and variables (the cyanobacterial mean abundance) can be extended through this origin.

For the analysis of the cyanobacterial morphotype data, the Cronbach's Alpha was 0.941, this factor meant this data set had 94.1 % reliability. This number is based on the total eigenvalue. The eigenvalue for dimension 1 was 5.111 and for dimension 2 was 2.817. The percent of variance for dimension 1 was 36.507 and for dimension 2 was 20.124.

The CATPCA ordination diagram for the cyanobacterial morphotype in each temperature range and season is shown in Figure 12. In dimension 1, *Synechococcus* cf. *lividus*, *Cyanothece* sp. and *Phormidium* cf. *boryanum* showed a strong negative correlation with others morphotypes. Three morphotypes had a close relationship to the distribution across the range of temperature, sites and seasons. They were found in higher range of temperature in all northern hot springs (Figure 13).

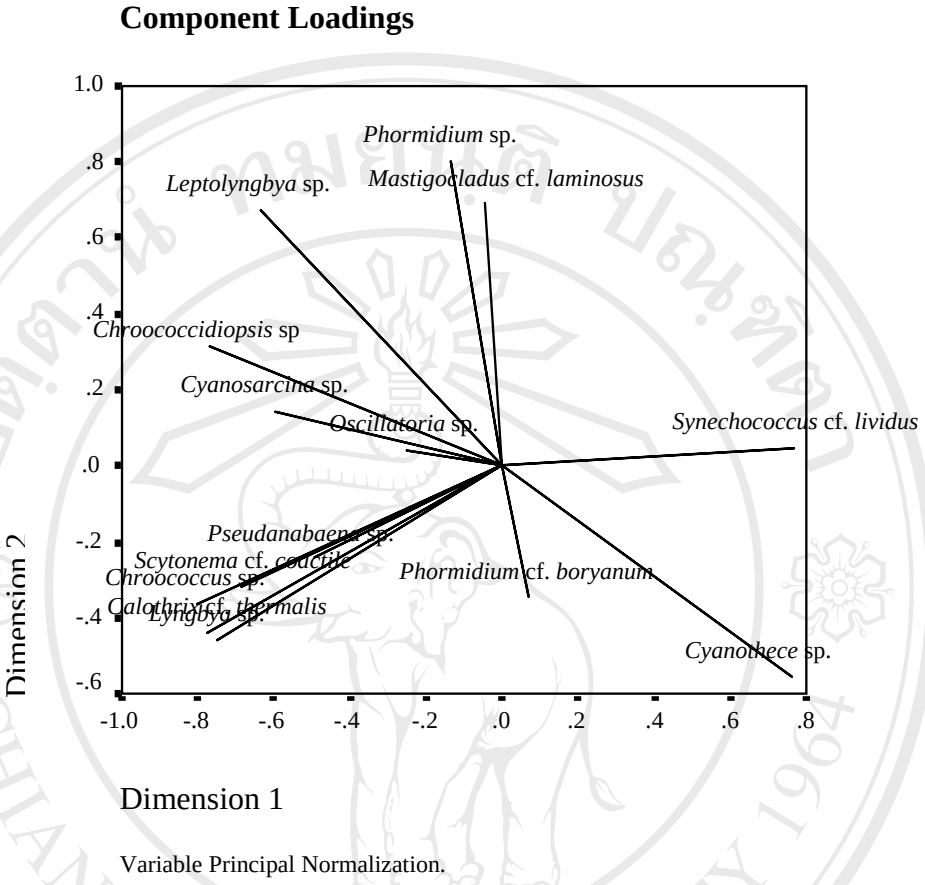

Figure 12. The ordination plot of cyanobacterial morphotypes presented in hot springs of each temperature range and season. This diagram represented component loadings (cyanobacterial morphotype).

The scatter plot of hot springs at each range of temperature and season is shown in Figure 13. The two groups of hot springs which had a close relationship, are mentioned into A and B. Group A represented the hot springs in northern Thailand in a high range of temperature from 50-75°C in every season, but SK was in the 45-50°C range in every season. Group B represented the hot springs in central and southern Thailand. They had close correlation within their groups.

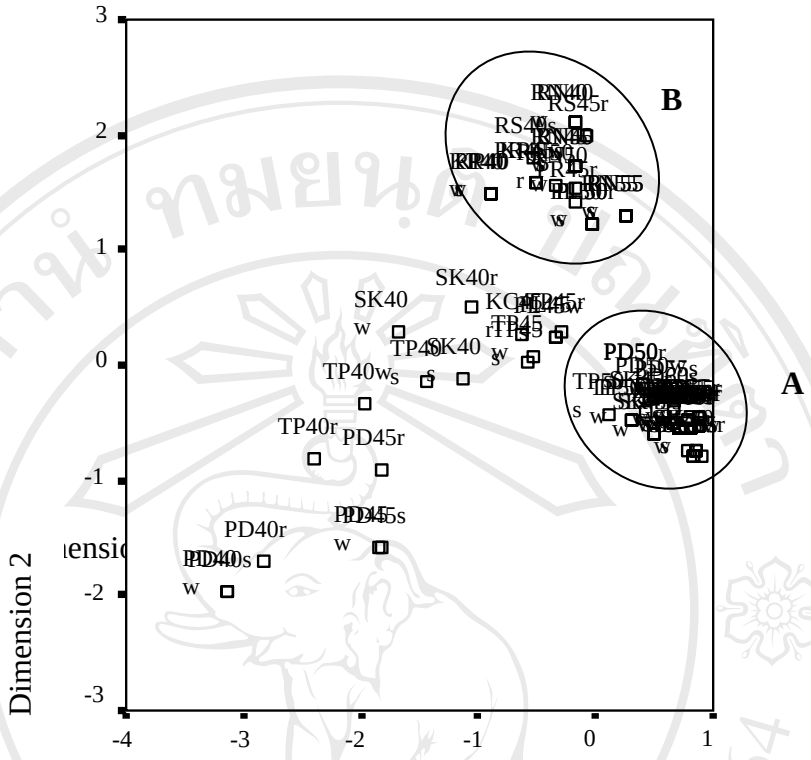

Variable Principal
Normalization.

Figure 13. The ordination plot of cyanobacterial morphotypes presented in hot springs of each temperature range and season. This diagram represents object points (hot springs of each temperature range and season).

CATPCA also generated a biplot, a useful extension of ordination diagram. This diagram contained two sets of data derived in rather different ways to assist in the interpretation of an ordination by highlighting relationships within the data (Shaw, 2003). The biplot ordination of cyanobacterial morphotypic abundance present within all six hot springs in each temperature range and season is shown in Figure 14. The result of this ordination is that the species or morphotypes which are presented in further distance from the center indicate relevant significance which may be more specific to sampling sites than other species which are shown closer to the center. From this ordination plot, three morphotypes in group A, *Synechococcus* cf. *lividus*,

Cyanothece sp. and *Phormidium* cf. *boryanum*, had a close relationship. They had a positive correlation with the hot springs in northern Thailand in a higher range of temperature from 50-75°C in every season or they are the dominant species found in these hot springs. From group B, the cases of hot springs in central and southern Thailand had highly correlated with *Phormidium* sp. and *Mastigocladus* cf. *laminosus*. Both species were found to be dominant in these hot springs and they could indicate relevant significance that may be specific to the sampling sites because they are presented in greater distance from the center.

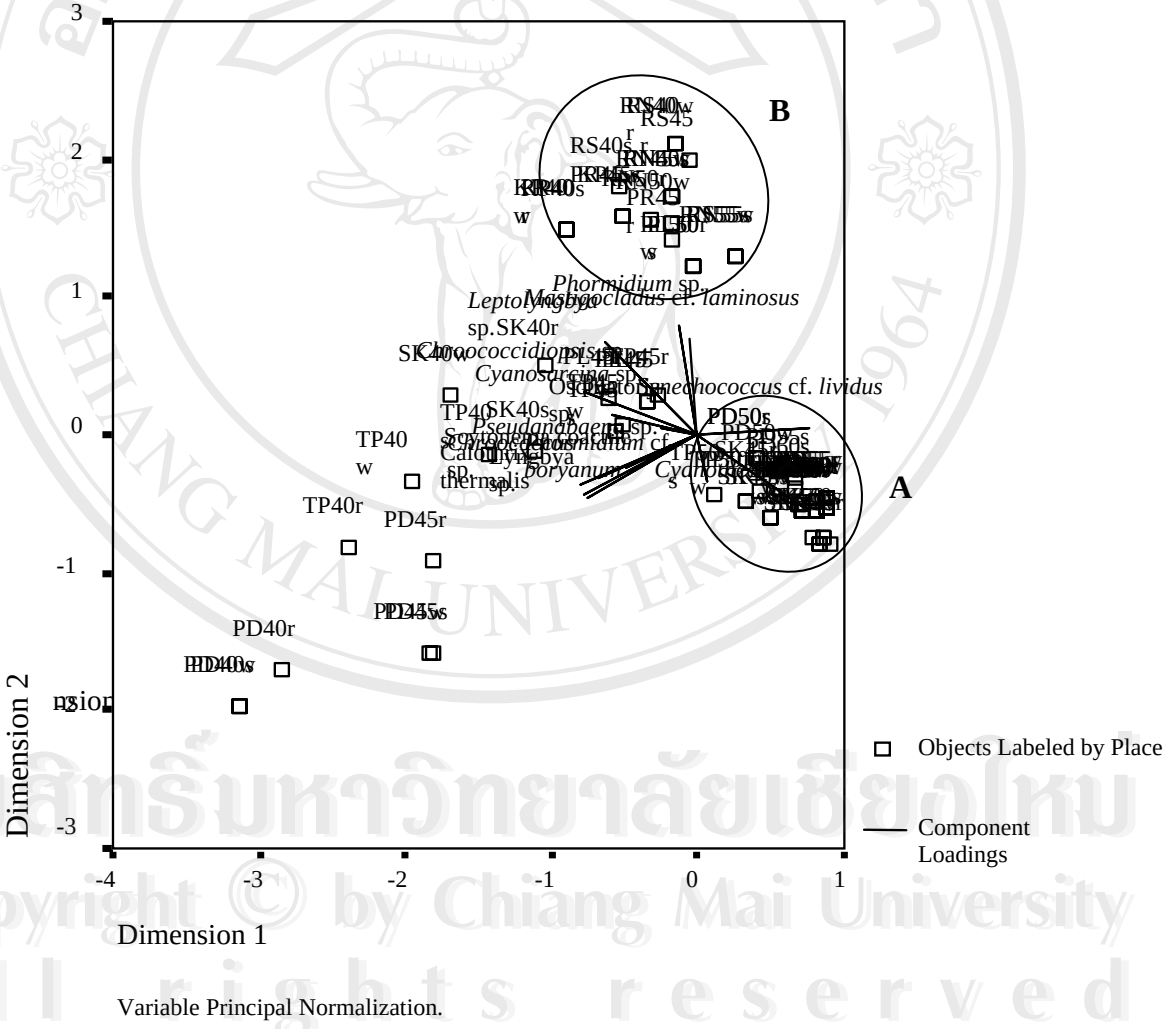

Variable Principal Normalization.

Figure 14. The CATPCA biplot ordination of the cyanobacterial morphotype data converted into a biplot by addition of lines showing morphotype loading.

4.3 Physico-chemical properties of all hot springs

The aquatic environments downstream of hot springs present well defined physico-chemical gradients with opportunities for niche colonization. The source water temperatures in this study ranged from almost 100 °C in all northern hot springs, but central and southern hot springs had the comparatively cool source water temperatures 50-60°C (Table 1). The seasonal variation of the source water temperature of each spring was less than 5°C (Figure 16). This constancy combined with the minor intra-annual variation in ambient temperature in this tropical region, suggested that the thermal gradient downstream of each spring was a stable and persistent physical feature of the environment (Sompong *et al*., 2005). However, the air temperature variation was high, up to 7-10°C in KC and PR Hot Springs (Figure 15). The seasonal variation in the source water temperature of KC and PR Hot Springs differed from all other hot springs in that the samples were collected over a different period (4 hour period) and were affected by sunlight.

The physico-chemical properties of the water in each sampling reach in each spring were measured in three seasons. The physico-chemical ranges across all sampling reaches at each spring are shown in Figures 17-30.

The pH of all hot springs was in the range of 7-9, which had an average pH of 7.87 (Figure 17). By the average pH, there was no significant difference between sampling sites and seasons.

The conductivity of all hot springs was in the high range from 474-2,190 μs/cm. The conductivity in three hot springs in northern Thailand was in the range from 520-1,120 μs/cm, but the conductivity of the southern hot springs was in the high range from 474-2,190 μs/cm, and the highest conductivity was at the RS Hot Spring (Figure 18). The conductivity at the RS and KC Hot Springs in cold dry season were high because of the dissolved ions from the surface water. The conductivity result depends on temperature and the dissolved ions or total component concentration in the water (Raksaskulwong, 2000). The conductivity in all hot springs was higher than natural cool water because it has been derived from surface water and rain, which then infiltrated through the ground and when the water received heat transfer from hot rocks. Then

heated up and became exposed to the surface. The ability of the heat transfer of hot water dissolved elements and ions (Raksaskulwong, 2000).

The alkalinity of all springs was in the range from 132 to 264 mg/l and had an average of 199.8 mg/l (Figure 19). The alkalinity is indicated from surface water and geological dissolved substances such as nutrient and inorganic carbon forms (Sanmanee, 1998).

The concentration of the dissolved nutrients [soluble reactive phosphorus (SRP) and inorganic forms of nitrogen (nitrate nitrogen and ammonium nitrogen)] were high in all the source waters (Figures 20-22). Maximum nitrate nitrogen, ammonium nitrogen and SRP at any site were 25.9, 2.38 and 1.68 mg/l, respectively. The highest concentration of nitrate nitrogen and ammonium nitrogen were found in SK Hot Spring and the highest concentration of SRP was found in TP Hot Spring. Minimum nitrate nitrogen, ammonium nitrogen and SRP of all sites were 0.7, 0 and 0.06 mg/l, respectively. The inorganic forms of nitrogen at SK Hot Spring were high in cold dry season because high inorganic forms of nitrogen in the surface water were mixed with the hot water and exposed to surface. Therefore, nutrients were unlikely to be important determinants of the horizontal spatial distribution or diversity of the cyanobacterial species.

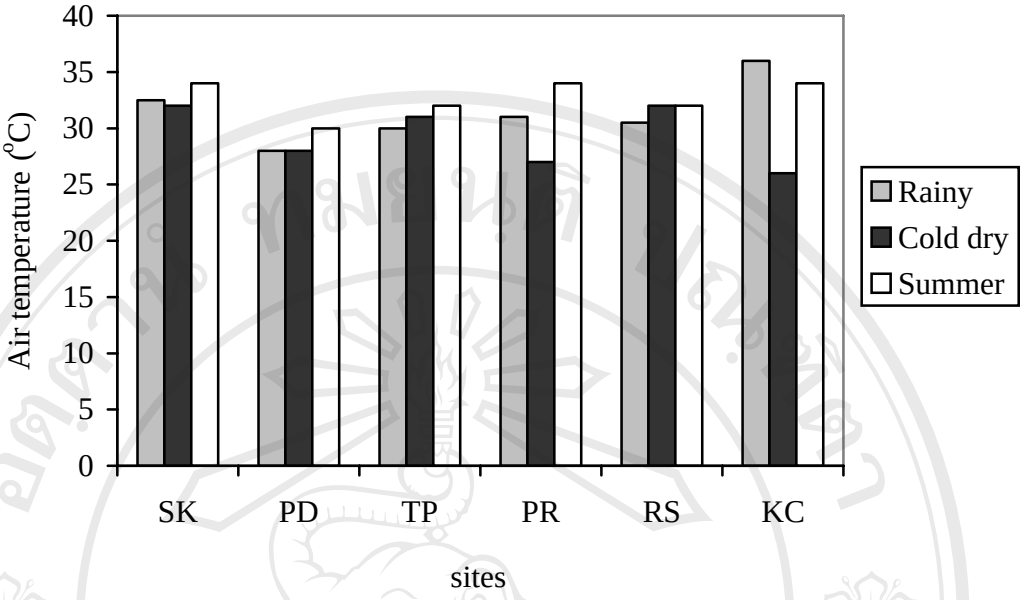

Figure 15. Air temperature of the 6 hot springs in rainy, cold dry and summer seasons

1. San Kamphaeng Hot Spring (SK)
2. Pong Dued Hot Spring (PD)
3. Theppanom Hot Spring (TP)
4. Pra Rueang Hot Spring (PR)
5. Raksawarin Public Park Hot Spring (RS)
6. Khaochaison Hot Spring (KC)

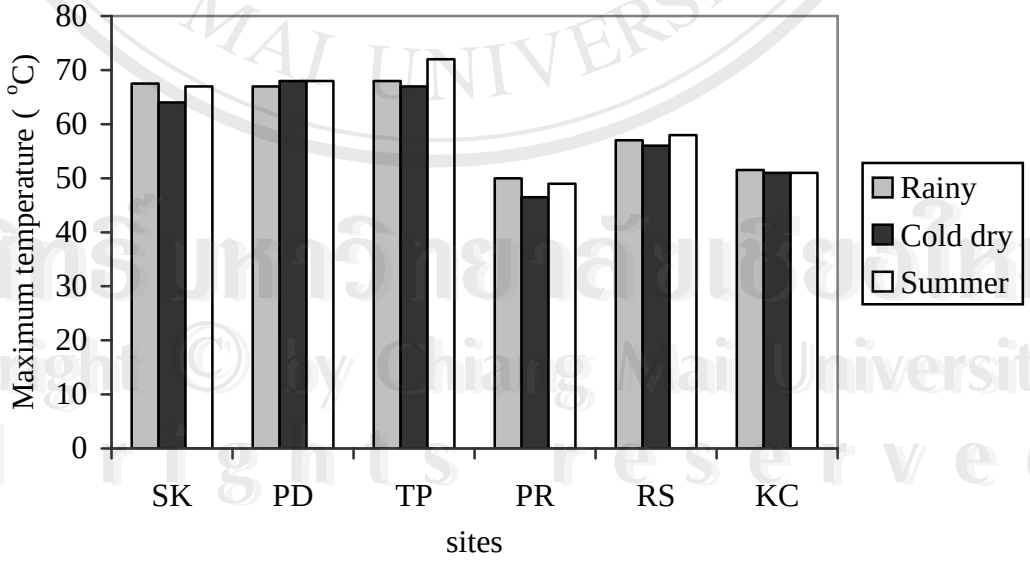

Figure 16. Maximum temperature of water in the 6 hot springs in rainy, cold dry and summer seasons

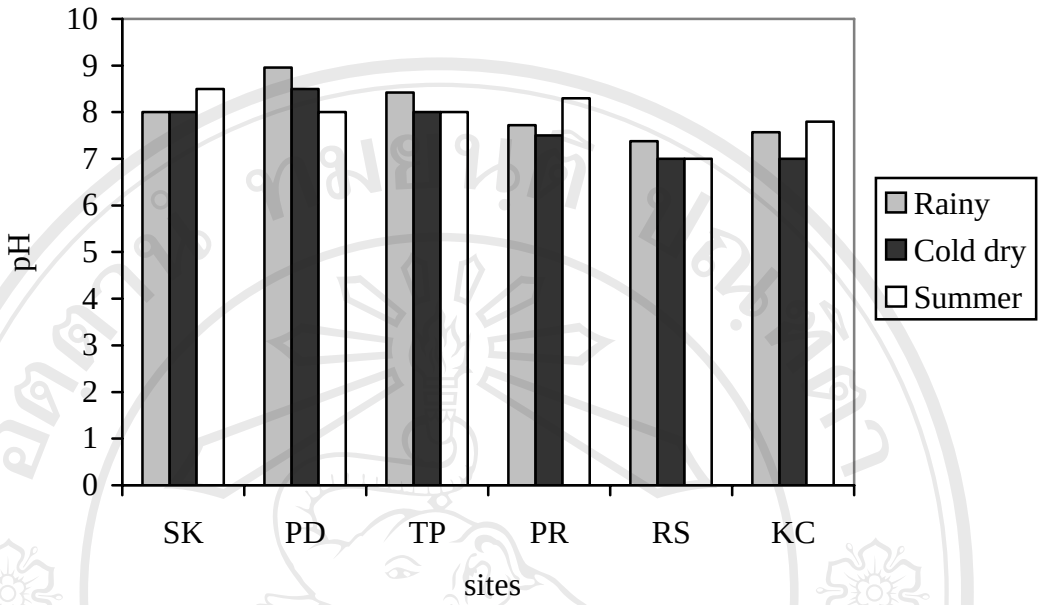

Figure 17. pH of water in the 6 hot springs in rainy, cold dry and summer seasons

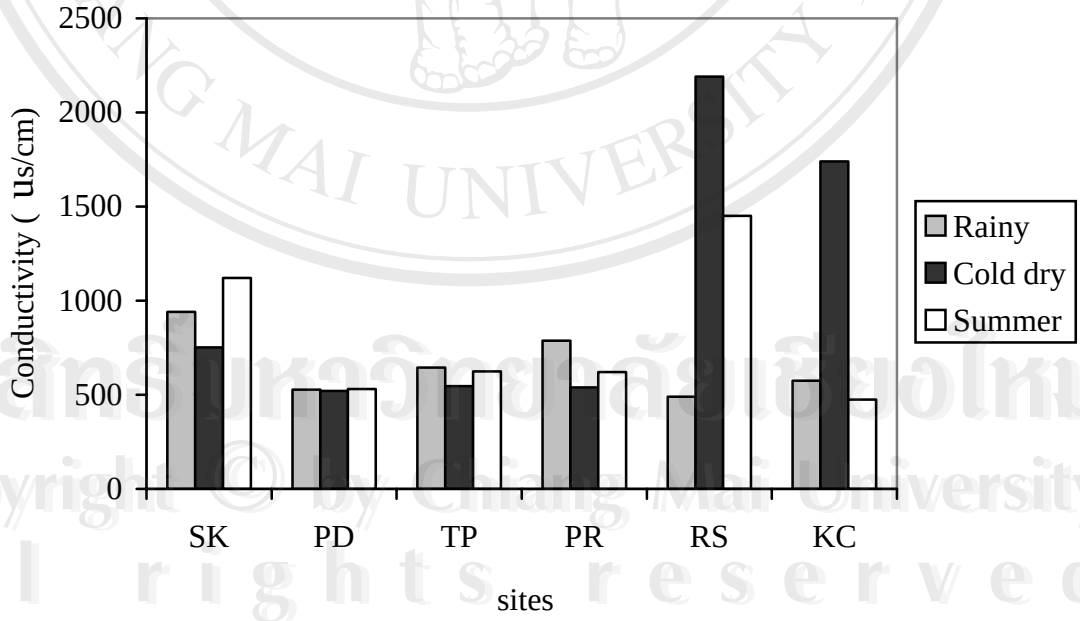

Figure 18. Conductivity of water in the 6 hot springs in rainy, cold dry and summer seasons

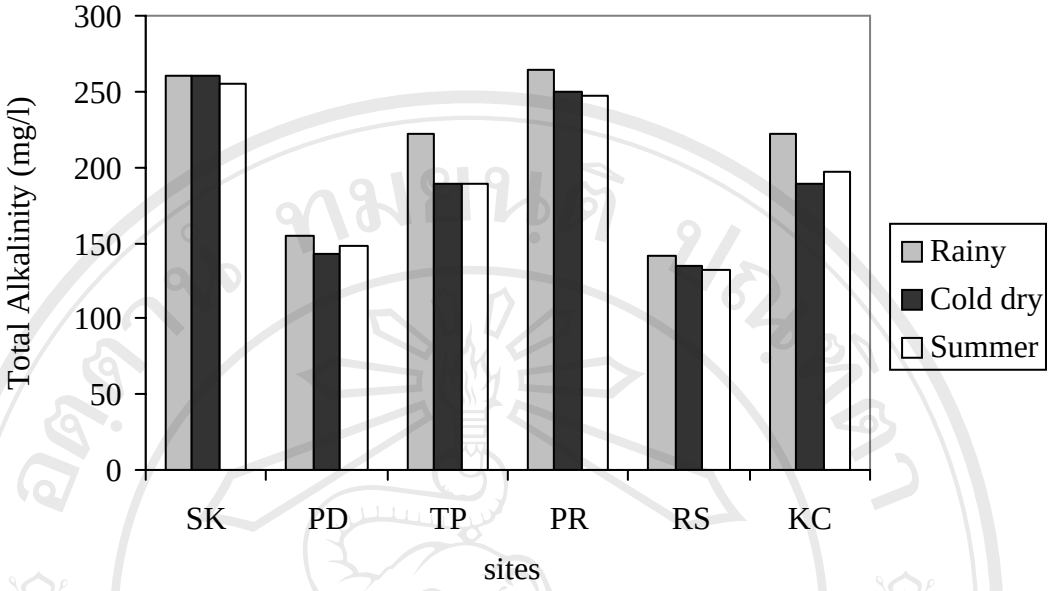

Figure 19. Total alkalinity of water in the 6 hot springs in rainy, cold dry and summer seasons

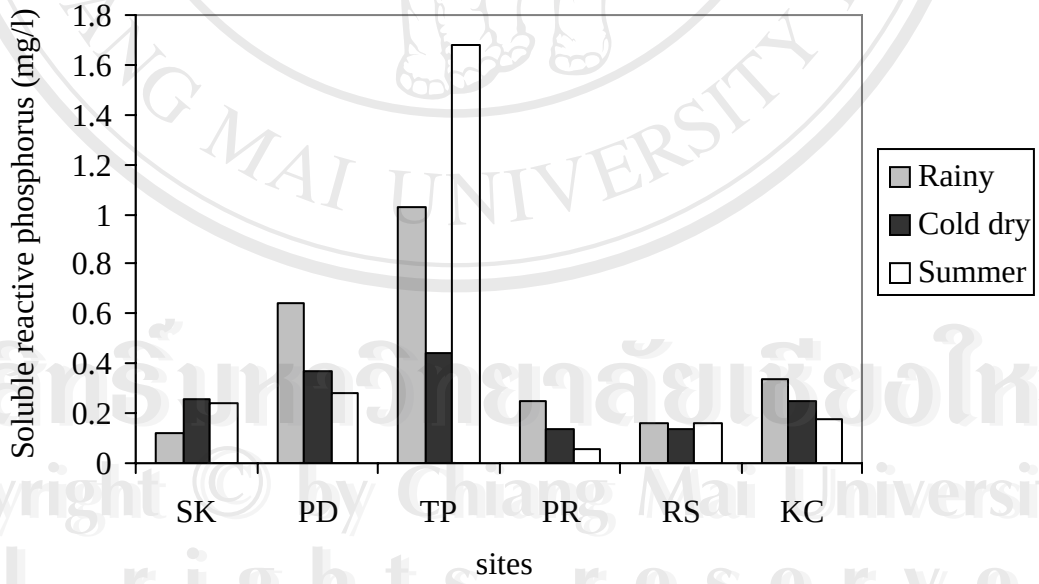

Figure 20. Soluble reactive phosphorus of water in the 6 hot springs in rainy, cold dry and summer seasons

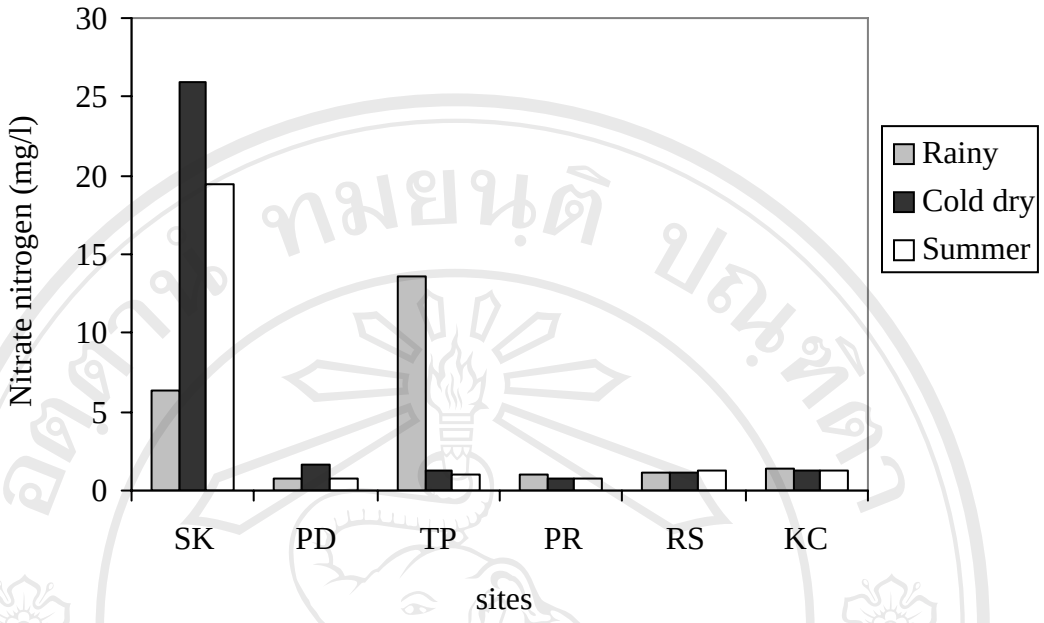

Figure 21. Nitrate nitrogen of water in the 6 hot springs in rainy, cold dry and summer seasons

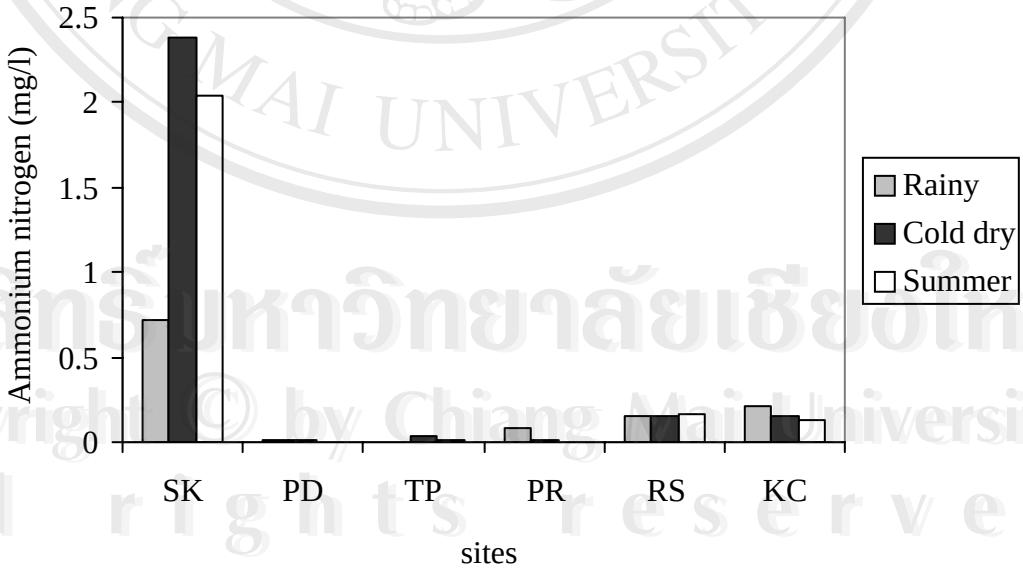

Figure 22. Ammonium nitrogen of water in the 6 hot springs in rainy, cold dry and summer seasons

Dissolved sulfide was present in the source waters of all northern hot springs. Its concentration was less or none in southern and central hot springs. Essentially, dissolved sulfide (20-40 mg/l) severely poisoned photosynthesis of nonadapted populations. However, a tolerant cyanobacterial species (*Oscillatoria amphigranulata* van Goor) was usually present in low to high sulfide levels (1-60 mg/l) (Castenholz, 1976; 1977). This species and another *Oscillatoria* could be able to utilize sulfide as a reductant in photosynthesis (Cohen *et al.*, 1975a; 1975b). The sulfide concentration declined downstream as the water was exposed to atmospheric oxygen (Sompong *et al.*, 2005). The highest sulfide level was at SK Hot Spring in summer (6.02 mg/l) (Figure 23). The maximum sulfide concentration in most other springs was 0.18 mg/l.

Another form of sulfur, sulfate, could be detected in the water. Cyanobacteria and other microorganisms use sulfate to produce protein to sustain their growth. Some anaerobes can use oxygen metabolite from sulfate (Sanmanee, 1998). Sulfate was present in the source waters of all hot springs. The highest sulfate level was at SK Hot Spring in the rainy season (220 mg/l) (Figure 24). The maximum sulfate concentration in most other springs and was 34 mg/l in TP Hot Spring. Dissolved sulfide and sulfate were high in SK Hot Spring because of the geological characteristics of the hot spring. It could be related to some active geologic fratures, lineations and granitic plutons of various ages (Bunopas and Vella, 1983; Raksaskulwong, 2000).

The water hardness has an effect on cations such as Ca^{2+} and Mg^{2+}. The source water of all hot springs has hardness, Ca^{2+} and Mg^{2+} values between 28-206, 6-64.13 and 1.95-34.16 mg/l, respectively (Figures 25-27). Such concentrations are not high when compared with other hot springs for instance Mammoth Hot Spring in Yellowstone National Park. These cations precipitate making the travertine-depositing (calcium carbonate deposit) hot spring (Castenholz, 1977). Other dominant cations are Na^{+} (25.93-181.25 mg/l) and K^{+} (1.71-11.30 mg/l) (Figures 28-29). Another cation, Fe^{3+} has less than 0.005 mg/l (data not shown). The predominant anions is chloride (Cl^{-}) having a concentration value between 6.8-22.8 mg/l (Figure 30).

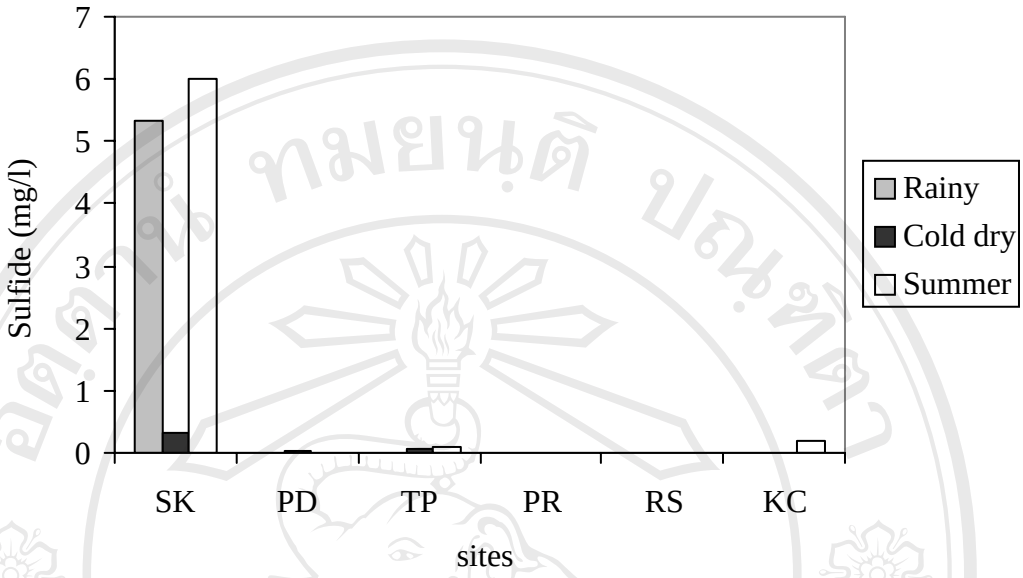

Figure 23. Sulfide of water in the 6 hot springs in rainy, cold dry and summer seasons

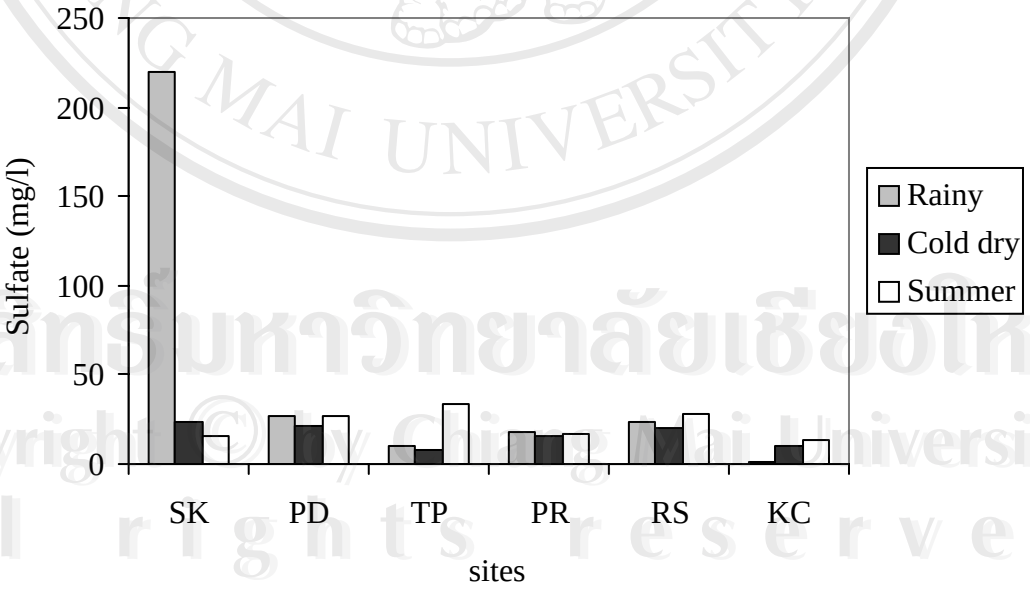

Figure 24. Sulfate of water in the 6 hot springs in rainy, cold dry and summer seasons

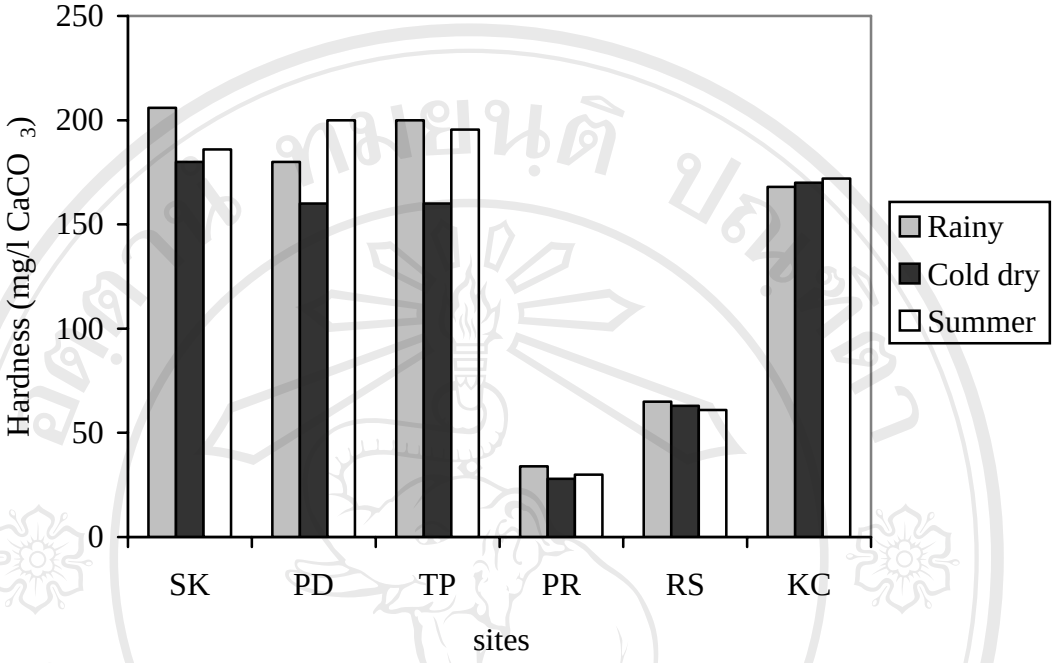

Figure 25. Hardness of water in the 6 hot springs in rainy, cold dry and summer seasons

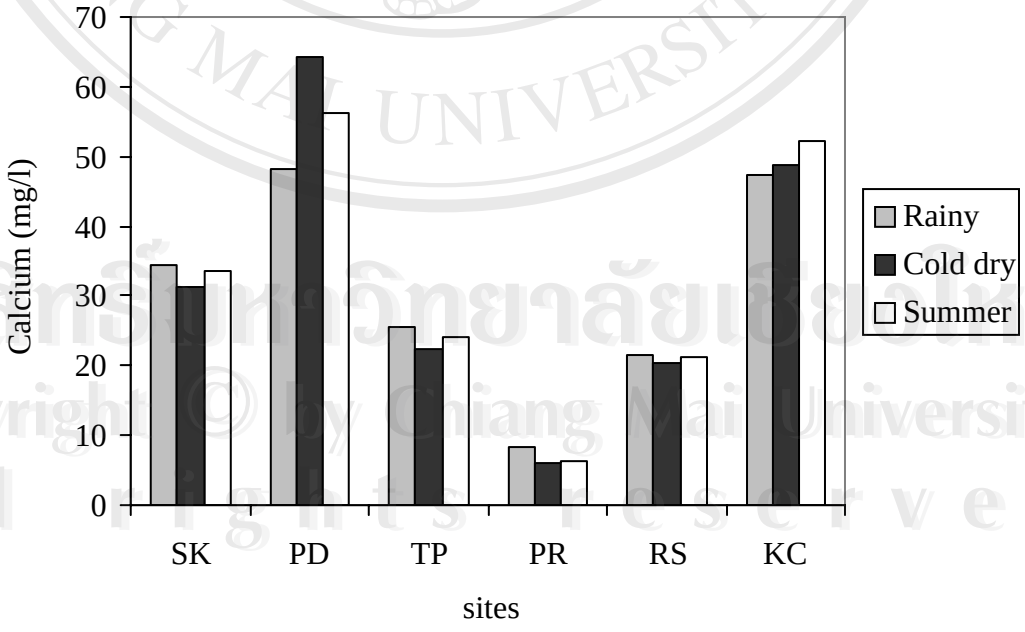

Figure 26. Calcium of water in the 6 hot springs in rainy, cold dry and summer seasons

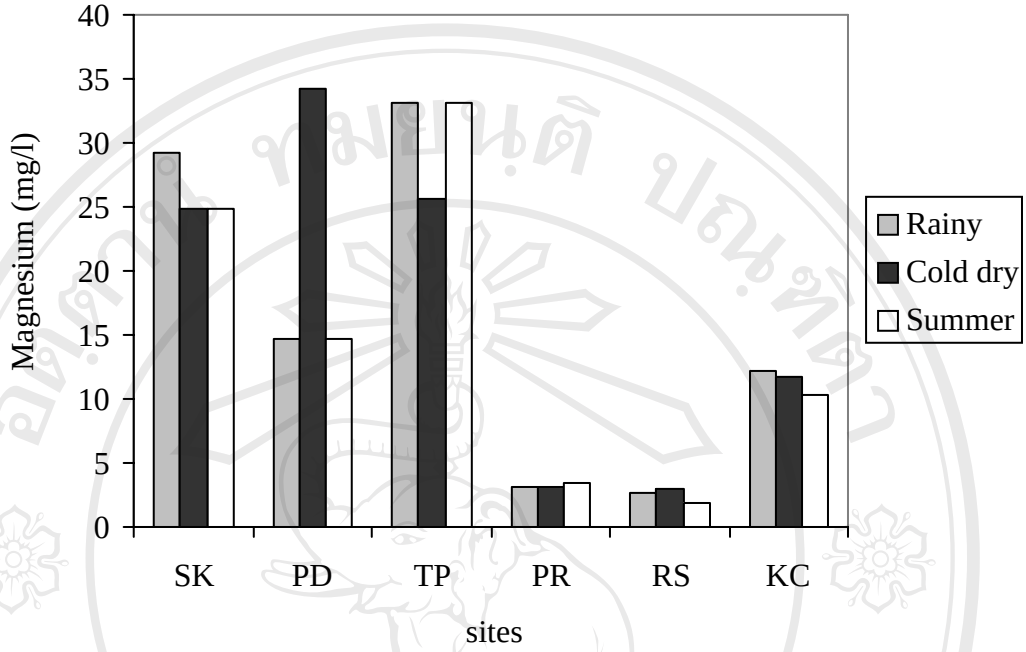

Figure 27. Magnesium of water in the 6 hot springs in rainy, cold dry and summer seasons

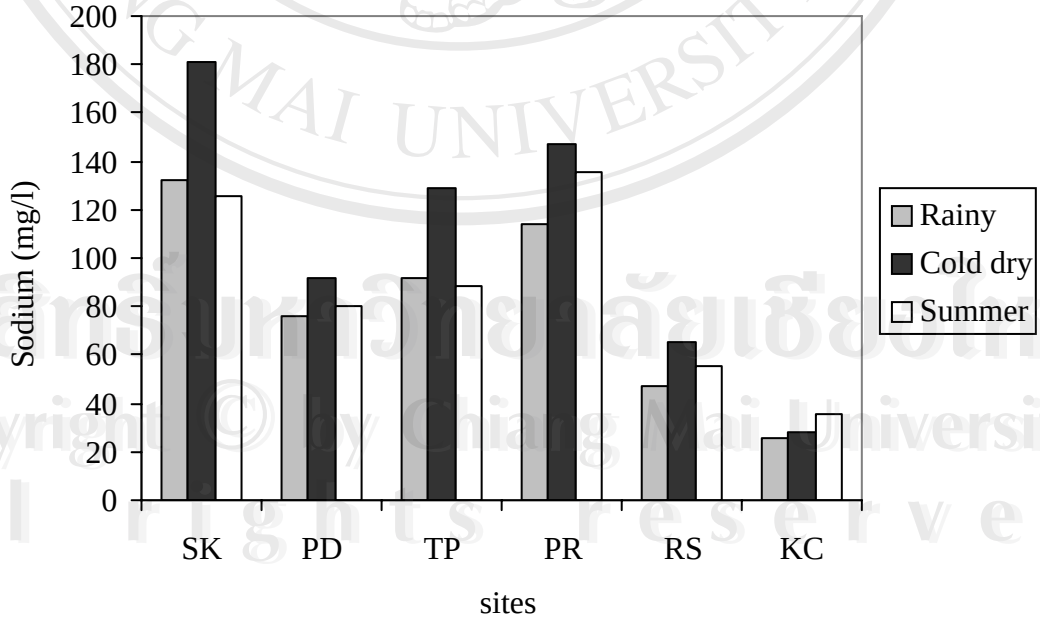

Figure 28. Sodium of water in the 6 hot springs in rainy, cold dry and summer seasons

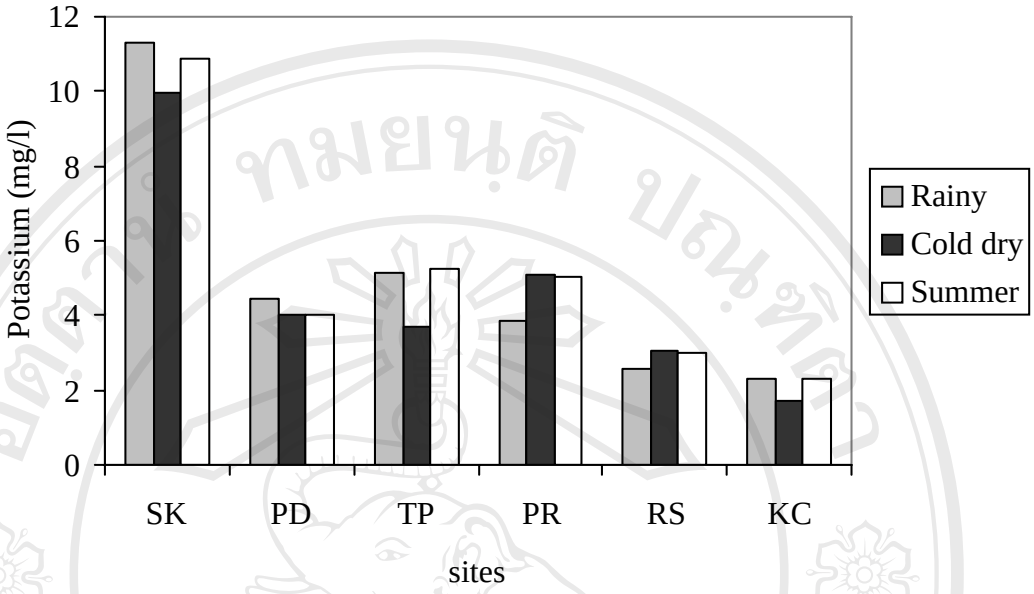

Figure 29. Potassium of water in the 6 hot springs in rainy, cold dry and summer seasons

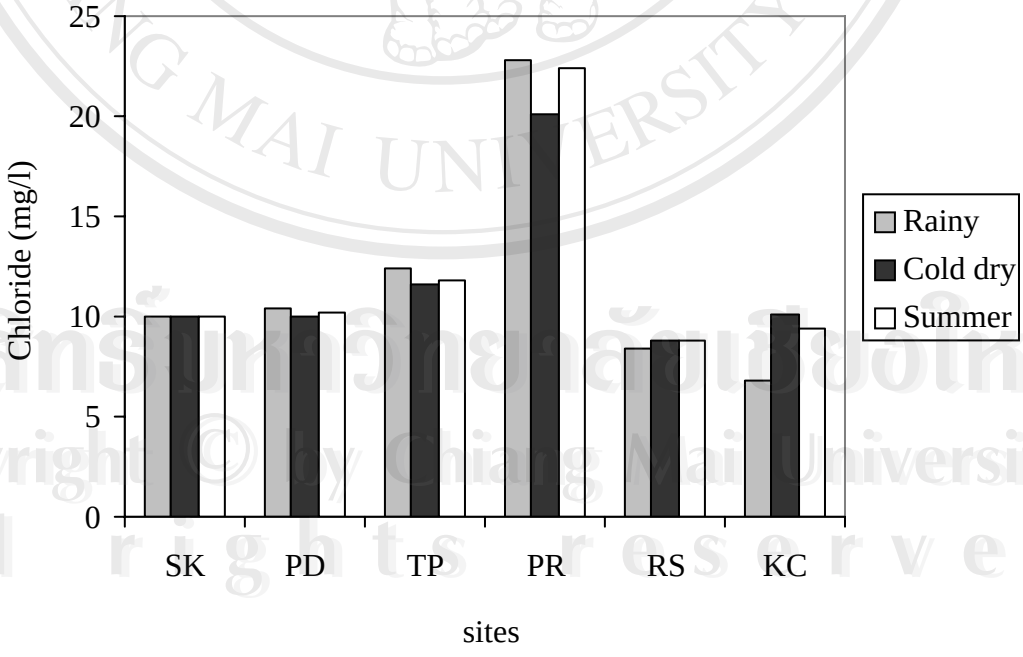

Figure 30. Chloride of water in the 6 hot springs in rainy, cold dry and summer seasons

4.4 Physico-chemical properties analysis

The physico-chemical parameters: maximum water temperature, pH, conductivity, total alkalinity, hardness, calcium, magnesium, sulfides, sulfate, soluble reactive phosphorus, nitrate nitrogen, ammonium nitrogen, sodium, potassium and chloride of all hot springs in each season were put into MVSP to perform statistical analysis: Principal Components Analysis (PCA) and Cluster Analysis of the correlation or relationship between all hot springs. Like all ordination techniques, PCA is a tool used to condense data. The output from the PCA is presented in ordination diagrams or two-dimensional scatterplot. The eigenvalue of the ordination axis in PCA is used to show how much variance is accounted for by the axis (Shaw, 2003). The graph plotted was the scattergraph of axis 1 against axis 2, this holds the greatest percentage of the overall variance. If the first two axes together account for 90% of the total variance in a multivariate dataset, the majority of the information content of the data could be seen in one graph.

For the analysis of the physico-chemical properties data, the eigenvalue for axis 1 was 311.453 and for axis 2 was 3.965. The cumulative percentage for both axes was 97.270, which indicates that two axes capture about 97% of total variance in the data set. The majority of the information content of the data could be described by using only the first axis.

The ordination diagram for the physico-chemical properties analysis is shown in Figure 31. All hot springs in each season were grouped into 2 groups. The first group consisted of SK Hot Spring in three seasons and other hot springs contained in another group. However, both groups were high suggesting a close relationship between all hot springs when considered with eigenvalue of the ordination.

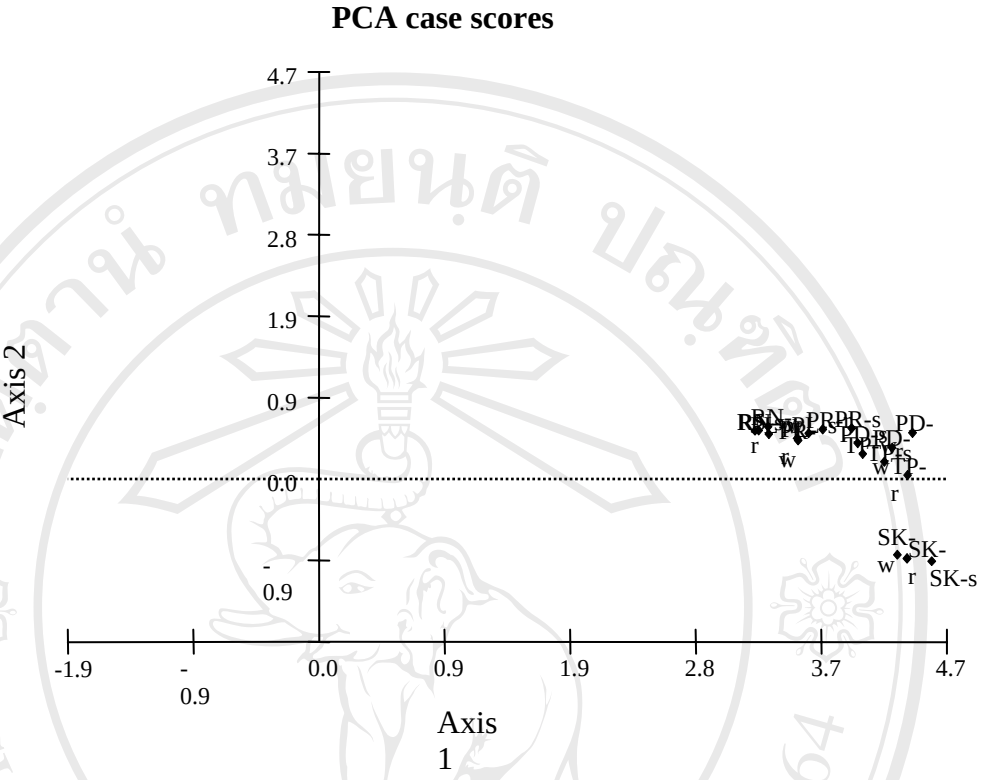

Figure 31. The PCA ordination diagram of the physico-chemical properties of all hot springs in each season.

The cluster analysis was computed by using MVSP. All physico-chemical properties of all hot springs in each season were put into this package and generated a dendrogram of relationship between the sampling sites, based on their similarities. The Euclidean distance index was used to find the distance between each pair of sites in the two-dimensional data space (Shaw, 2003). The UPGMA were used to make clustering algorithms. The data was transformed to Log_{10}. All hot springs in each season were grouped into 2 clusters (Figure 32). The first group was divided into 2 subgroups; subgroup 1.1 consisted of PR and RS Hot Springs in all three seasons and subgroup 1.2 consisted of KC and PD Hot Springs in all three seasons and TP Hot Spring in cold dry and summer season. The second group was divided into 2 subgroups; subgroup 2.1 consisted of TP Hot Spring in rainy season, SK Hot Spring in summer and cold dry seasons and subgroup 2.2 consisted of SK Hot Spring in rainy season.

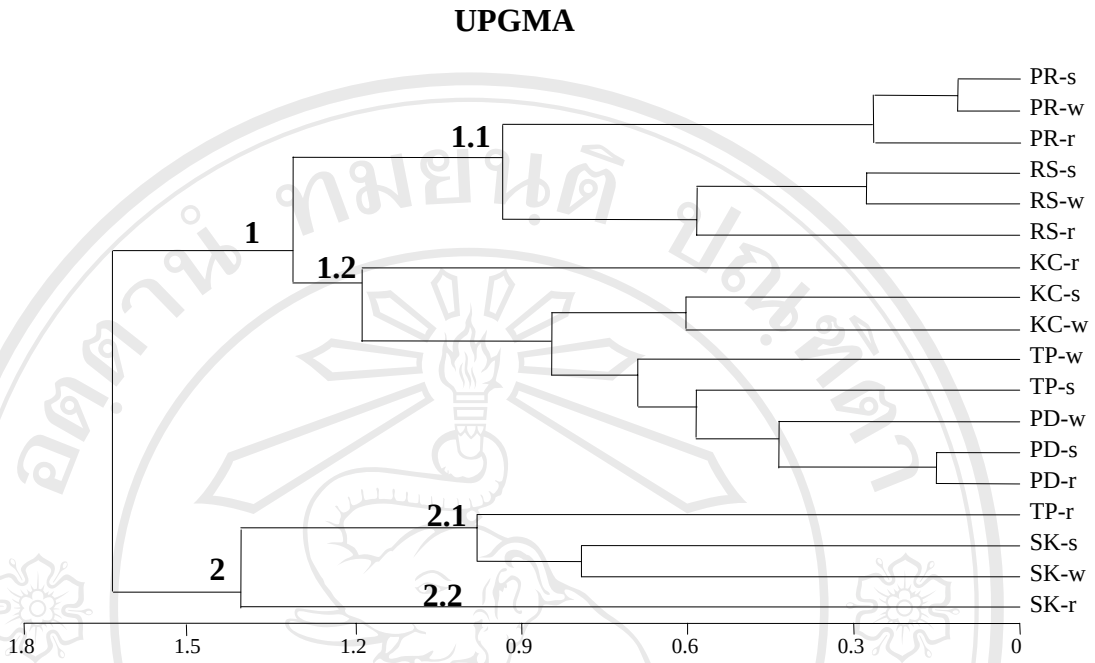

Figure 32. The UPGMA cluster analysis of the physico-chemical properties of all hot springs in each season.

From the dendrogram of UPGMA cluster analysis, each hot spring were grouped when considered two major groups of the dendrogram, except for TP Hot Spring, which were divided into 2 groups: TP-r was divided into group 2 and TP-w and TP-s were divided into group 1. This dendrogram had a result similar with the PCA ordination diagram in Figure 31, which were divided into 2 groups.

4.5 Canonical correspondence analysis (CCA) of physico-chemical properties and cyanobacterial morphotype data of all hot springs

The result of the CCA is presented in an ordination dendrogram. It is computed from the combination of environmental or physico-chemical factors and cyanobacterial morphotypes. The environmental arrows represent the direction of maximum change in the value of variables. The angle between two arrows (axes) indicates the correlation

between the length of the arrow which is equal to the maximum rate of the variable. Variables with long arrows do vary much in the data set and have a strong influence on community structure. The morphotypes or species are presented in points. The position of which is based on their distribution in relation to the environmental variables (Ter Braak, 1986). From the dendrogram, the species which are presented in greater distance from the center indicate relevant significance which may be specific to sampling sites than the other species which are closer to the center.

For the CCA analysis of the cyanobacterial morphotype data, the eigenvalue for axis 1 was 0.076 and for axis 2 was 0.017. The cumulative percentage for both axes was 36.865 or about 37% of total variance in the data set. The morphotype species-environmental correlation for CCA axis 1 (0.954) and axis 2 (0.841) suggests a close relationship between the pattern of morphotypic abundance and physico-chemical variables (Figure 33). The ordination diagram for the morphotype analysis is shown in Figure 33. From this dendrogram, *Mastigocladus* cf. *laminosus* was high, significantly correlated to a high conductivity. This variable showed a negative correlation with other factors (which are closely related to each other). Nine morphotype points are positioned to the left of axis 1, where we found relatively high alkalinity, pH and hardness and high concentrations of sodium, magnesium, potassium, calcium, SRP, nitrate, ammonium, dissolved sulfide and sulfate.

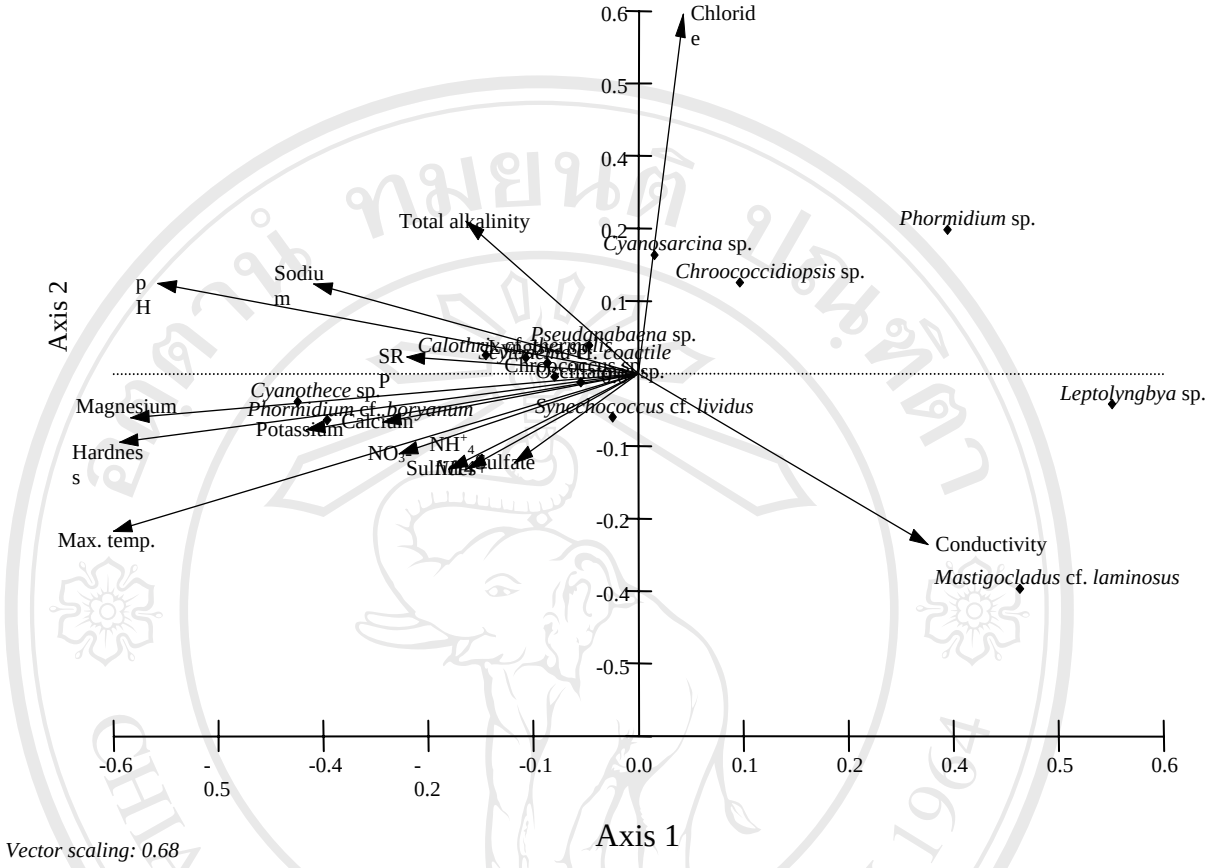

Figure 33. The CCA ordination diagram of the cyanobacterial morphotype data and physico-chemical properties of all hot springs in each season.

The ordination diagram for sampling sites is shown in Figure 34. This diagram shows central and southern hot springs which are positioned to the right of axis 1. All sampling sites in RS Hot Spring were high significantly correlated with high conductivity. These sampling sites showed a negative correlation with other sampling sites from northern hot springs. Sampling sites of SK Hot Spring had relatively high concentrations of dissolved sulfide and sulfate.

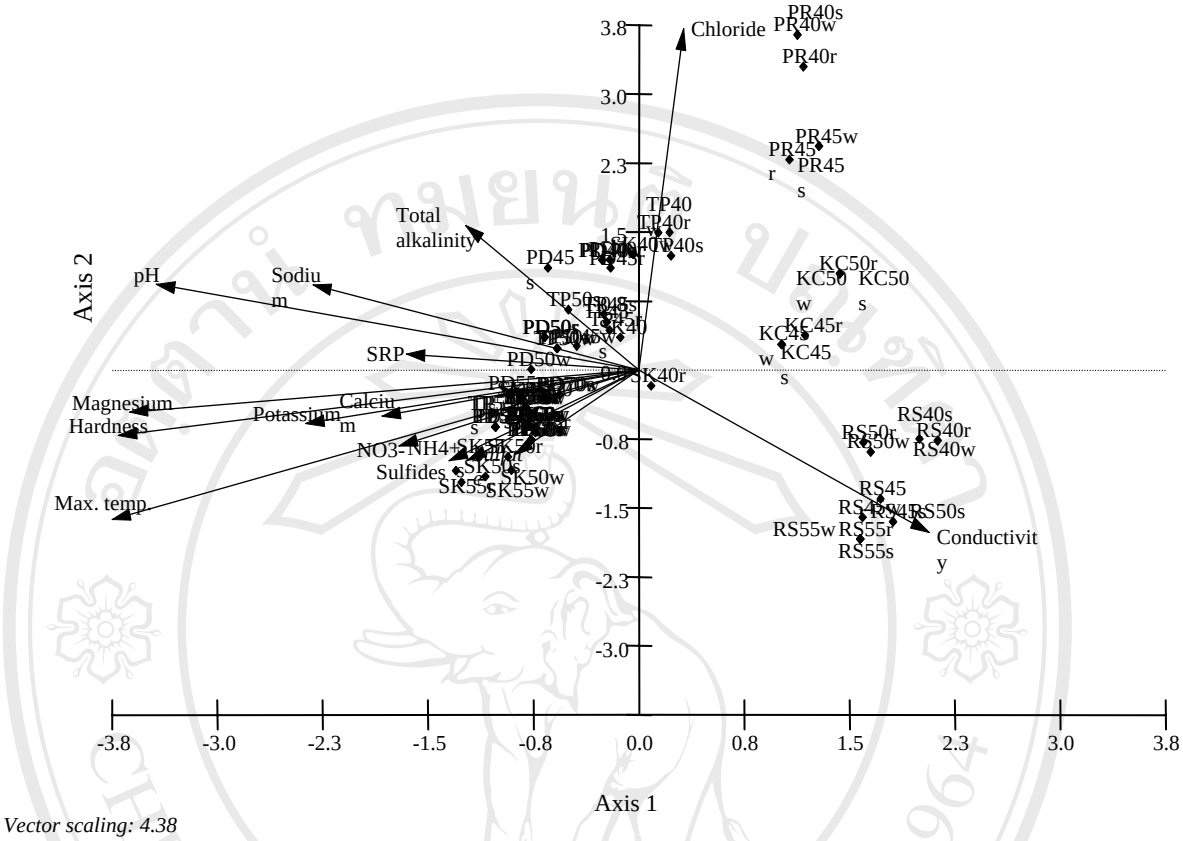

Figure 34. The CCA ordination diagram of the sampling sites when using cyanobacterial morphotype data and physico-chemical properties of all hot springs in each season.

4.6 Cyanobacterial enrichment cultures

For the enrichment cultures, not all of the cyanobacteria could be grown in the medium used. Although, a total of 55 clones of cyanobacteria were grown, *Synechococcus* spp., *Chroococcidiopsis* spp., *Leptolyngbya* spp., *Oscillatoria* spp., *Mastigocladus* spp., *Scytonema* spp. and *Phormidium* spp. were conspicuous in all samples (Appendix B). Some of the other dominant species, such as other strains of *Synechococcus, Cyanothece* and *Phormidium* cf. *boryanum,* were not successfully cultured and therefore were identified using the denaturing gradient gel electrophoresis (DGGE) analysis.

4.7 Molecular diversity of cyanobacterial 16S rRNA genes

To characterize those species of cyanobacteria that was not able to culture in the laboratory, we studied the 16S rRNA gene-defined community diversity in cyanobacterial mats from the six hot springs, using DGGE. A representative sample of DGGE separation of bulk cyanobacterial 16S rDNA is presented in Figures 35-40. Bands that migrated to the same position in the DGGE gel and displayed no ambiguous differences in nucleotide sequences were considered to represent unique 16S rDNA sequence types. Occasionally, some bands appeared to be heteroduplex molecules. Such bands form during mixed-template PCR when annealing occurs between similar but non-identical products (Ferris and Ward, 1997). The original heteroduplex products may then have reformed, migrating higher in the gradient, since base pair mismatches weaken hydrogen bonding between the double strands (Janse *et al.*, 2004).

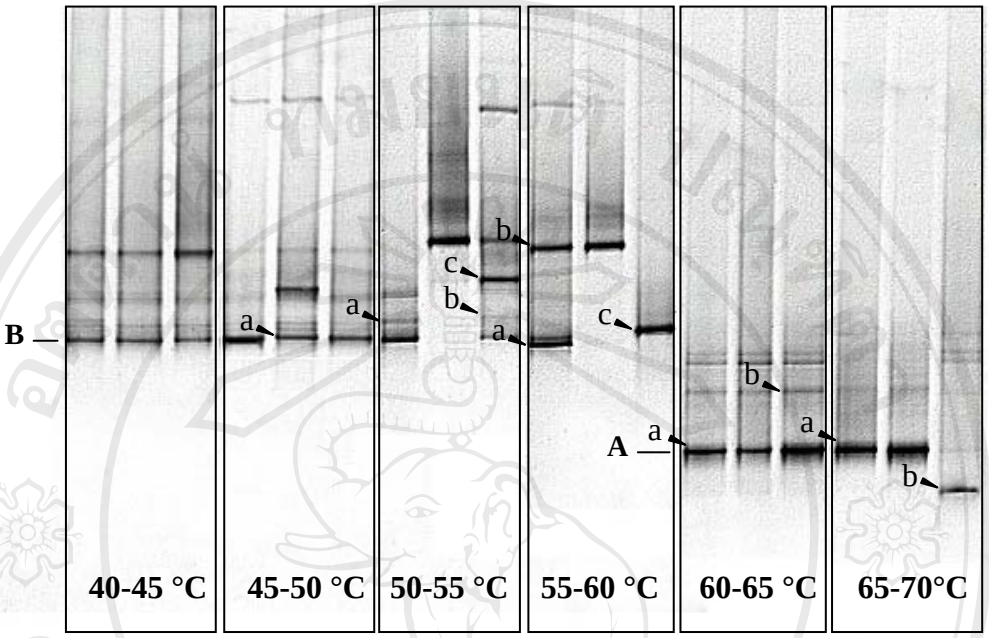

Figure 35. DGGE banding patterns of 16SrRNA gene-defined diversity among thermophilic cyanobacterial mats in San Kamphaeng (SK) Hot Spring. The first lane of each temperature range contains cyanobacterial mats from the rainy season, the second lane is from the cold dry season, and the third lane is from the summer season. Arrowheads to the left of the band indicate positions in the gradient at which defined bands were excised. For each temperature range, at each site, excised bands are labeled as lower case letters (abc). Conserved bands found across multiple temperature ranges or intervals are labeled with capital letters (AB).

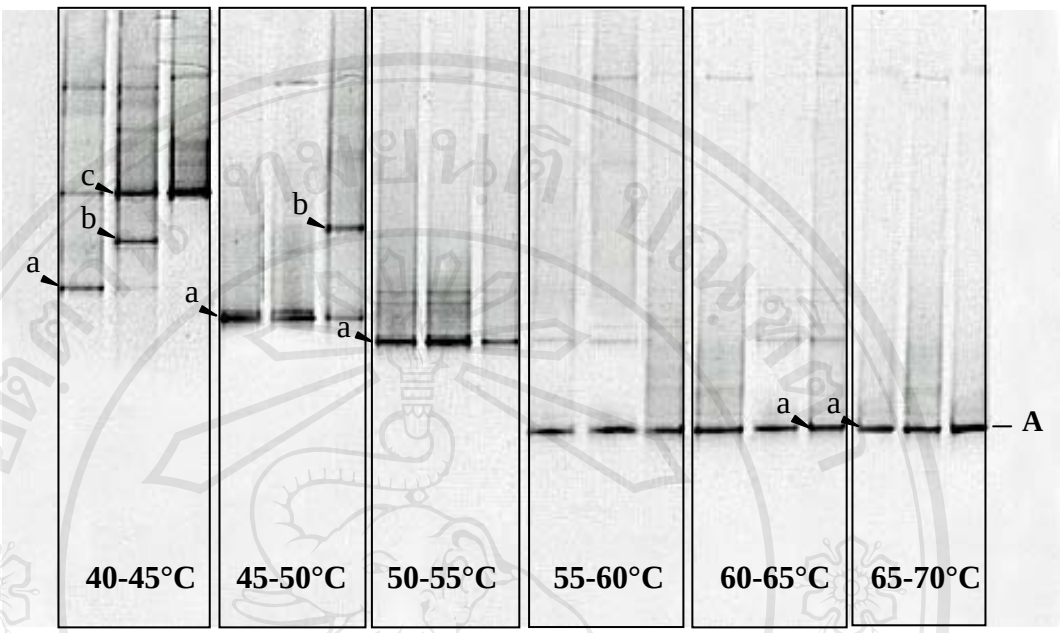

Figure 36. DGGE banding patterns of 16SrRNA gene-defined diversity among thermophilic cyanobacterial mats in Pong Dued (PD) Hot Spring. The first lane of each temperature range contains cyanobacterial mats from the rainy season, the second lane is from the cold dry season, and the third lane is from the summer season. Arrowheads to the left of the band indicate positions in the gradient at which defined bands were excised. For each temperature range, at each site, excised bands are labeled as lower case letters (abc). Conserved bands found across multiple temperature ranges or intervals are labeled with capital letter A.

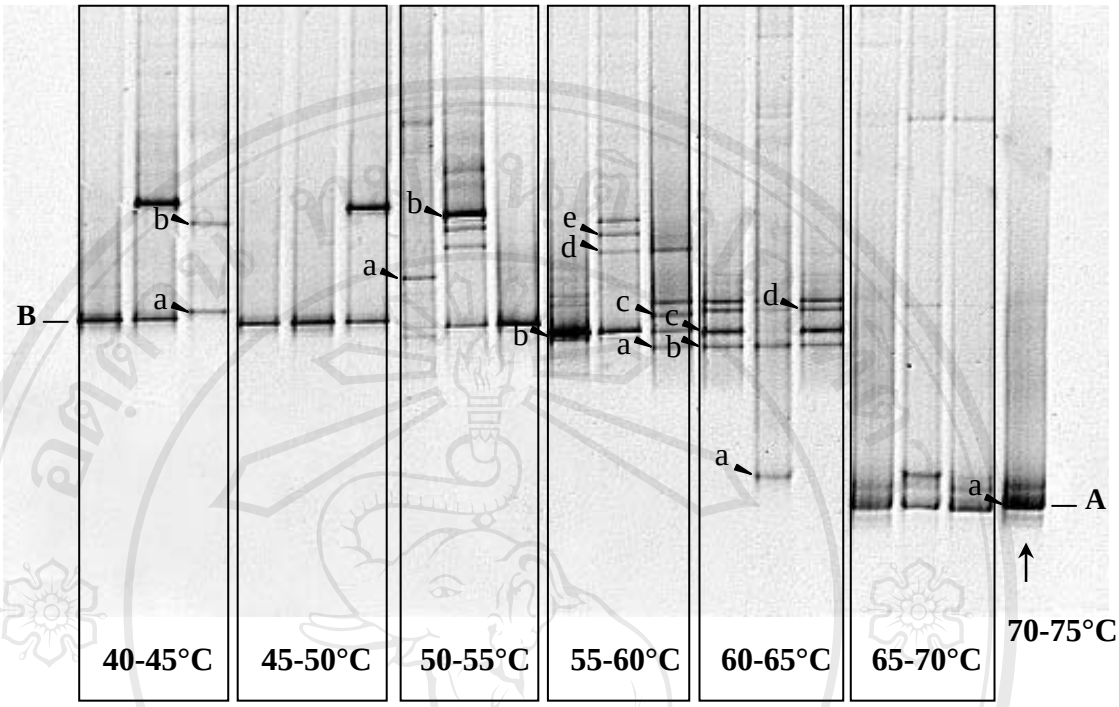

Figure 37. DGGE banding patterns of 16SrRNA gene-defined diversity among thermophilic cyanobacterial mats in Theppanom (TP) Hot Spring. The first lane of each temperature range contains cyanobacterial mats from the rainy season, the second lane is from the cold dry season, and the third lane is from the summer season. Arrowheads to the left of the band indicate positions in the gradient at which defined bands were excised. For each temperature range, at each site, excised bands are labeled as lower case letters (abcde). Conserved bands found across multiple temperature ranges or intervals are labeled with capital letters (AB).

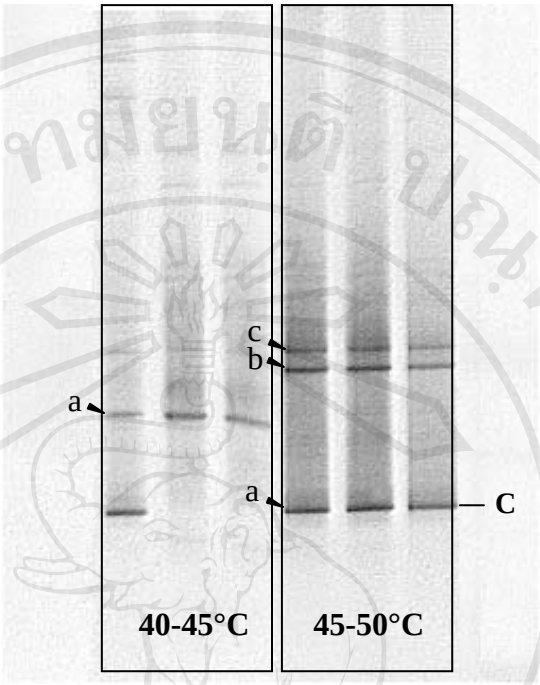

Figure 38. DGGE banding patterns of 16SrRNA gene-defined diversity among thermophilic cyanobacterial mats in Pra Rueang (PR) Hot Spring. The first lane of each temperature range contains cyanobacterial mats from the rainy season, the second lane is from the cold dry season, and the third lane is from the summer season. Arrowheads to the left of the band indicate positions in the gradient at which defined bands were excised. For each temperature range, at each site, excised bands are labeled as lower case letters (abc). Conserved bands found across multiple temperature ranges or intervals are labeled with capital letter C.

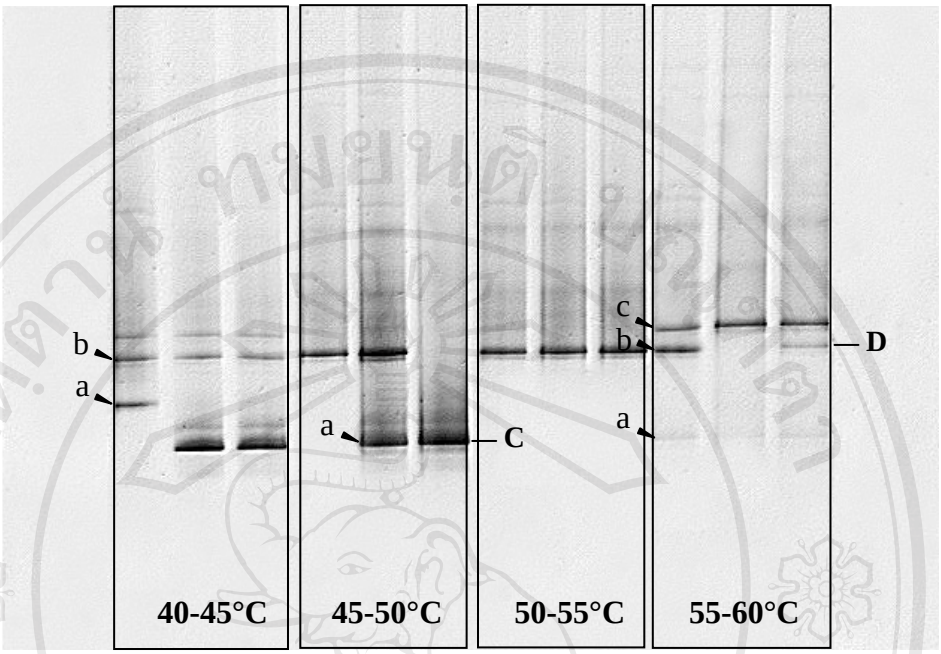

Figure 39. DGGE banding patterns of 16SrRNA gene-defined diversity among thermophilic cyanobacterial mats in Raksawarin Public Park (RS) Hot Spring. The first lane of each temperature range contains cyanobacterial mats from the rainy season, the second lane is from the cold dry season, and the third lane is from the summer season. Arrowheads to the left of the band indicate positions in the gradient at which defined bands were excised. For each temperature range, at each site, excised bands are labeled as lower case letters (abc). Conserved bands found across multiple temperature ranges or intervals are labeled with capital letters (CD).

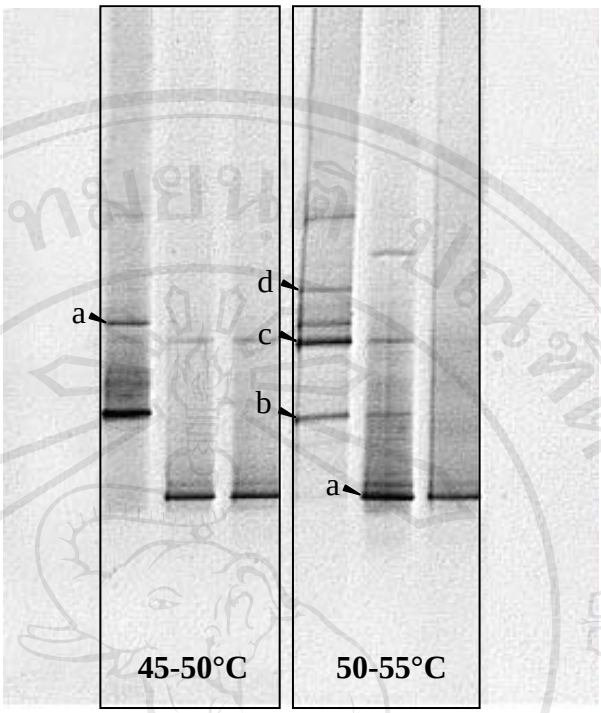

Figure 40. DGGE banding patterns of 16SrRNA gene-defined diversity among thermophilic cyanobacterial mats in Khaochaison (KC) Hot Spring. The first lane of each temperature range contains cyanobacterial mats from the rainy season, the second lane is from the cold dry season, and the third lane is from the summer season. Arrowheads to the left of the band indicate positions in the gradient at which defined bands were excised. For each temperature range, at each site, excised bands are labeled as lower case letters (abcd).

In general, band intensity should be indicative of the original abundance of the template DNAs in the original extractable population. Therefore, in this experiment, DNA loading concentration of each sample was set at 100-120 ng for loading into each lane. Although some factors, such as the G+C content of the sample DNA, primer specificity, and the presence of target sequences not complementary to the primers could still cause bias (Garcia-Pichel *et al*., 2001).

A total of 80 samples of DGGE amplified by PCR from environmental DNA samples were used with 37 bands then reamplified and sequenced. Most regions were sequenced directly from excised bands, but some samples that generated ambiguous sequences were cloned before sequencing. Two major bands, intense band A (Figures 35, 36, 37) from the high temperature intervals and band B (Figures 35, 37) from the moderate temperature intervals were conspicuous in three northern hot springs (SK, PD and TP). For two of the other major bands, intense band C (Figure 38, 39) was conspicuous in only the PR and KC hot springs and band D (Figure 39) was conspicuous in only the RS hot spring. Essentially all banding patterns were similar from different seasons within the same springs with the possible exceptions being Pong Dued (PD) at 40-45ºC, Theppanom (TP) at 55-60ºC and Khaochaison (KC) at 45-50ºC.

4.8 DGGE banding patterns of 16S rRNA gene analysis

The DGGE banding patterns of cyanobacterial 16SrRNA gene analysis of all hot springs in each season were put into MVSP to perform PCA analysis. The PCA analysis of DGGE banding patterns is presented in ordination diagrams or two-dimensional scatterplot. It showed the relationship between DGGE banding distribution in different ranges of temperature and seasons of all hot springs. The ordination diagram for the DGGE banding patterns of San Kamphaeng Hot Spring is shown in Figure 41. The eigenvalue for axis 1 was 4.558 and for axis 2 was 3.614. The cumulative percentage for both axes was 60.790, which indicates that the two axes capture about 61% of the total variance in the data set.

The PCA scatter plot (Figure 41) shows the relationship between DGGE banding distribution in different ranges of temperature and seasons. It was found that the DGGE

profile in this hot spring was different between temperature ranges but not different in each season. They were defined by 2 groups; the first group consisted of 2 temperature ranges (60-65, 65-70°C) in all three seasons and another group contained other sampling points in 4 other temperature ranges (40-45, 45-50, 50-55 and 55-60°C).

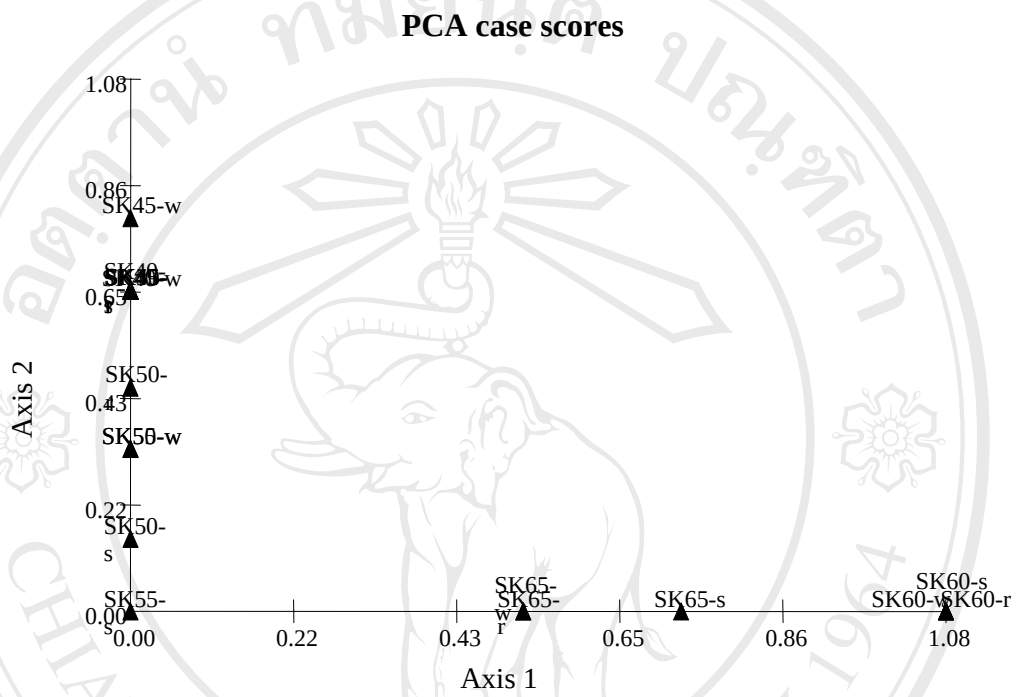

Figure 41. PCA ordination diagram of cyanobacterial DGGE profile distribution in San Kamphaeng Hot Spring.

The ordination diagram for the DGGE banding patterns of Pong Dued Hot Spring is shown in Figure 42. The eigenvalue for axis 1 was 2.489 and for axis 2 was 2.304. The cumulative percentage for both axes was 42.921, which indicates that the two axes capture about 43% of the total variance in the data set.

From the PCA scatter plot (Figure 42), it was found that the DGGE profile in this hot spring was different between temperature ranges but not different in each season. They are defined by 3 groups; the first group consisted of 4 temperature ranges (50-55, 55-6060-65, 65-70°C) in all three seasons, the second group consisted of the sampling points in the 45-50°C temperature range and the third group consisted of the sampling points in the 40-45°C temperature range (graph not shown).

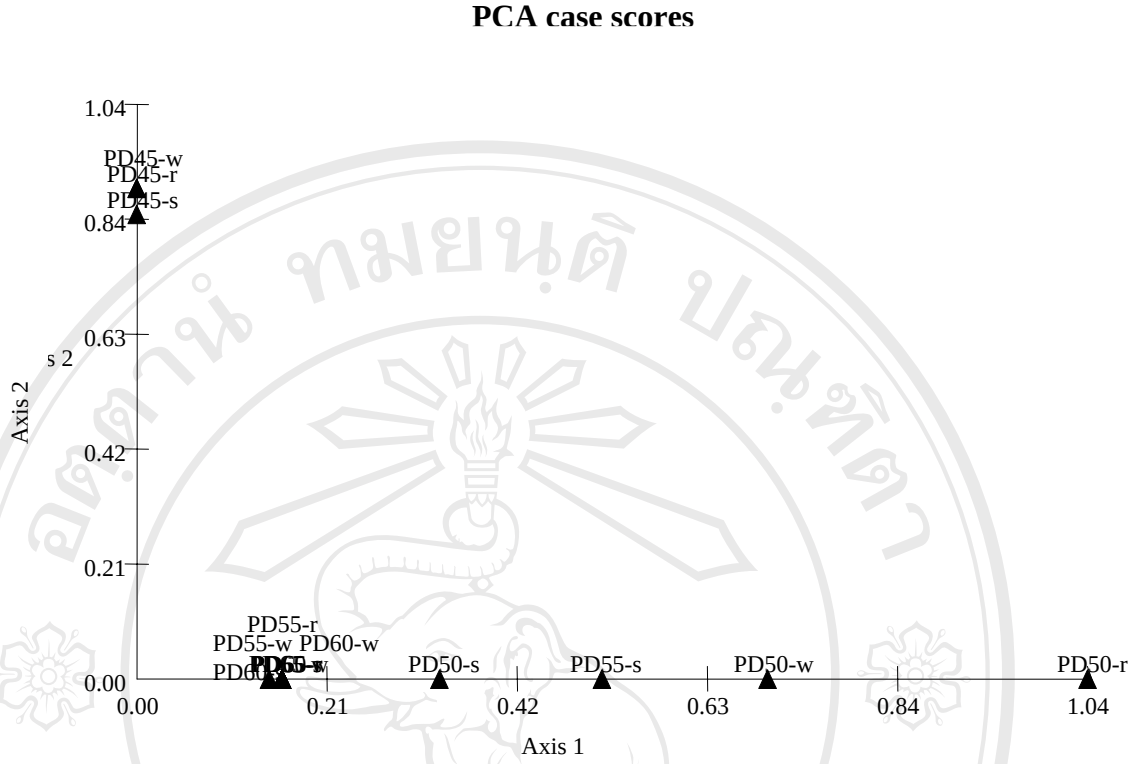

Figure 42. PCA ordination diagram of cyanobacterial DGGE profile distribution in Pong Dued Hot Spring.

The ordination diagram for the DGGE banding patterns of Theppanom Hot Spring is shown in Figure 43. The eigenvalue for axis 1 was 5.905 and for axis 2 was 2.825. The cumulative percentage for both axes was 50.256, which indicates that the two axes capture about 50% of the total variance in the data set.

From the PCA scatter plot (Figure 43), it was found that the DGGE profile in this hot spring was not clearly different between temperature ranges and seasons. All sampling points are included in the one group. Most of sampling points have a positive correlation with axis 1. However, four of the sampling points, TP50-w, TP55-w, TP60-r and TP60-s, have a positive correlation with both axis 1 and 2.

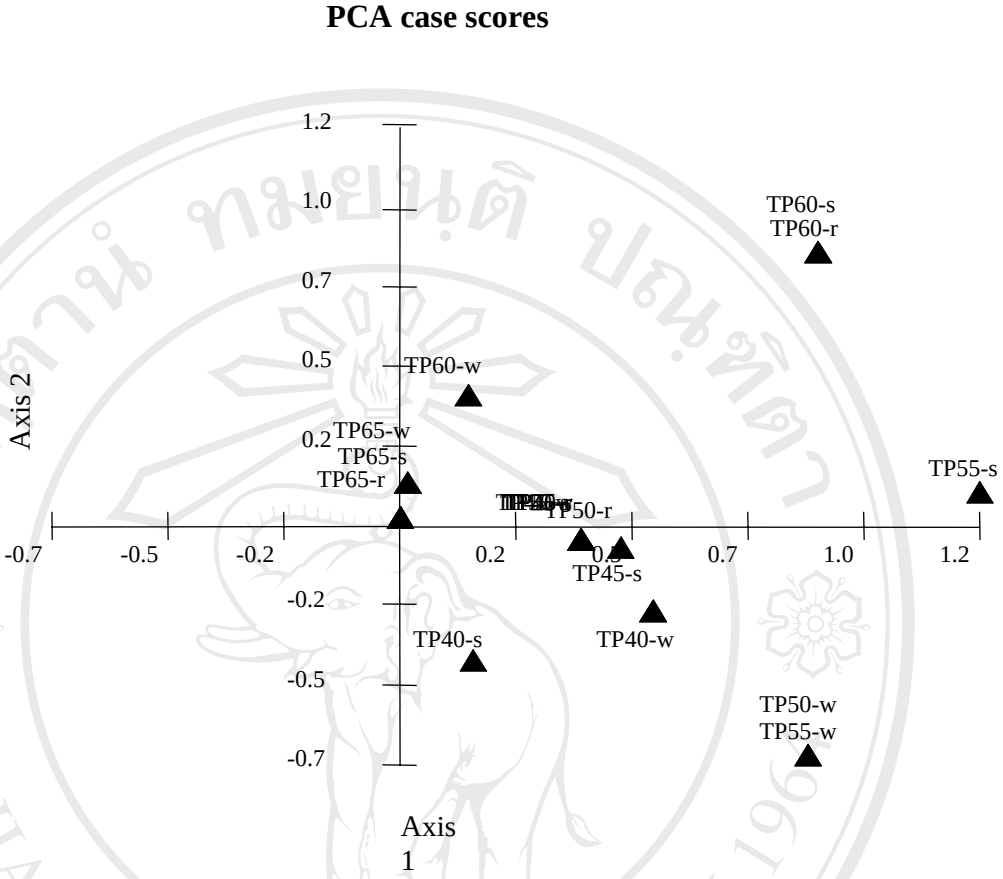

Figure 43. PCA ordination diagram of cyanobacterial DGGE profile distribution in Theppanom Hot Spring.

The ordination diagram for the DGGE banding patterns of Pra Rueang Hot Spring is shown in Figure 44. The eigenvalue for axis 1 was 4.791 and for axis 2 was 2.000. The cumulative percentage for both axes was 97.018.

From the PCA scatter plot (Figure 44), it was found that the DGGE profile in this hot spring was different for each temperature range. They are defined by 2 groups; the first group consists of 40-45°C temperature range in all three seasons, which have a positive correlation with axis 2, and another group which contains the 45-50°C temperature ranges and have a positive correlation with axis 1.

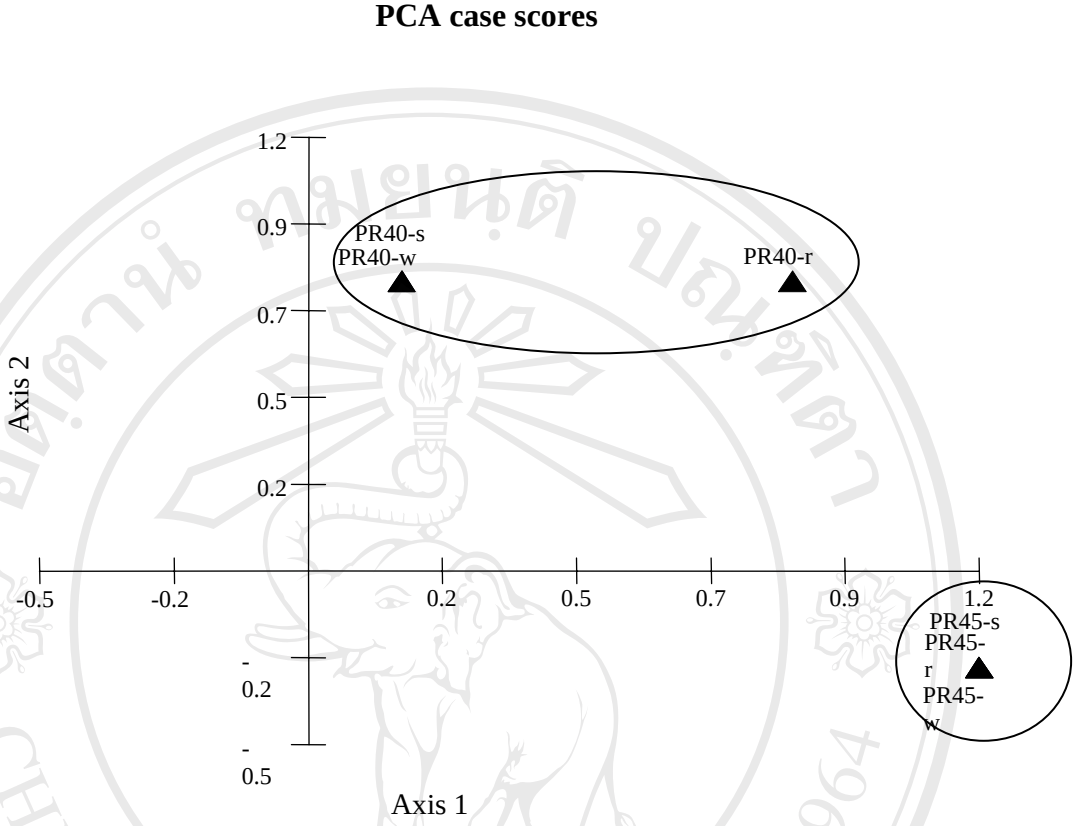

Figure 44. PCA ordination diagram of cyanobacterial DGGE profile distribution in Pra Rueang Hot Spring.

The ordination diagram for the DGGE banding patterns of Raksawarin Public Park Hot Spring is shown in Figure 45. The eigenvalue for axis 1 was 8.413 and for axis 2 was 1.673. The cumulative percentage for both axes was 87.773.

From the PCA scatter plot (Figure 45), it was found that the DGGE profile in this hot spring could be defined into 2 groups. The first group consisted of RS45-s (45-50°C temperature range in the summer season) and RS55-w (55-60°C temperature range in cold dry season), and another group which contains other sampling points, and have a positive correlation with axis 1. However, it was not clearly different between temperature ranges and each season.

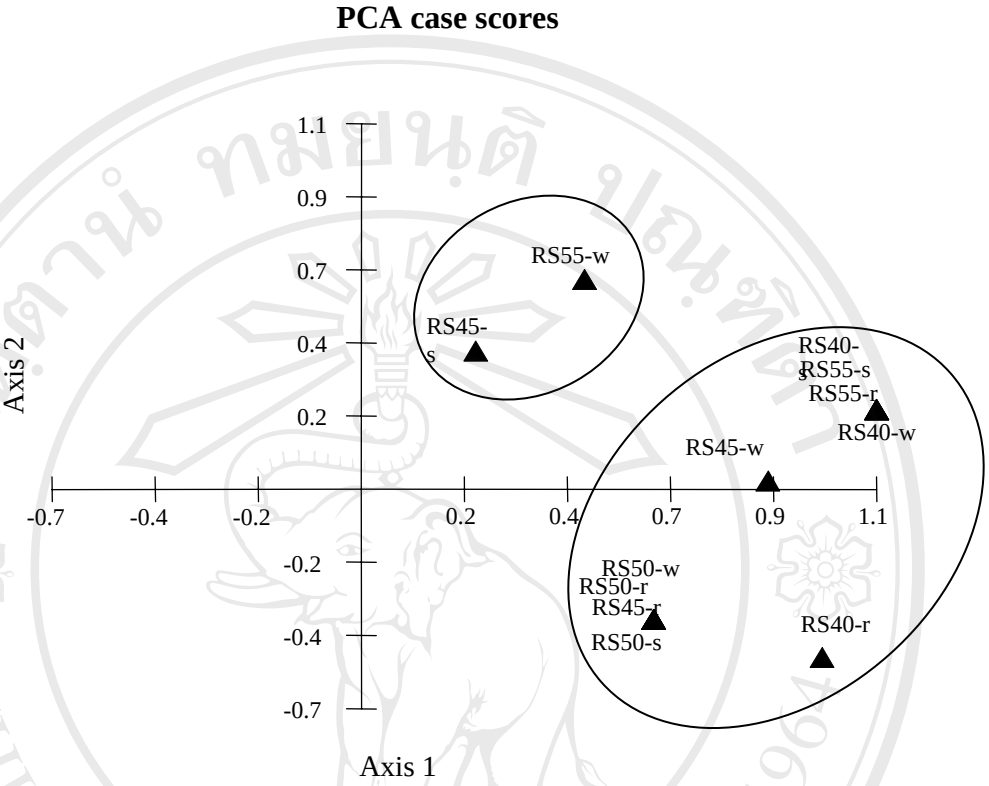

Figure 45. PCA ordination diagram of cyanobacterial DGGE profile distribution in Raksawarin Public Park Hot Spring

The ordination diagram for the DGGE banding patterns of Khaochaison Hot Spring is shown in Figure 46. The eigenvalue for axis 1 was 8.608 and for axis 2 was 3.791. The cumulative percentage for both axes was 90.502, which indicates that the two axes capture about 90% of the total variance in the data set.

From the PCA scatter plot (Figure 46), it was found that the DGGE profile in this hot spring was different in each season within each temperature range. They are divided into 2 groups; the first group consists of both temperature ranges in rainy season (45-50 and 50-55°C) and a have positive correlation with axis 2, and another group contains other sampling points in the cold dry and summer seasons, which have a positive correlation with axis 1.

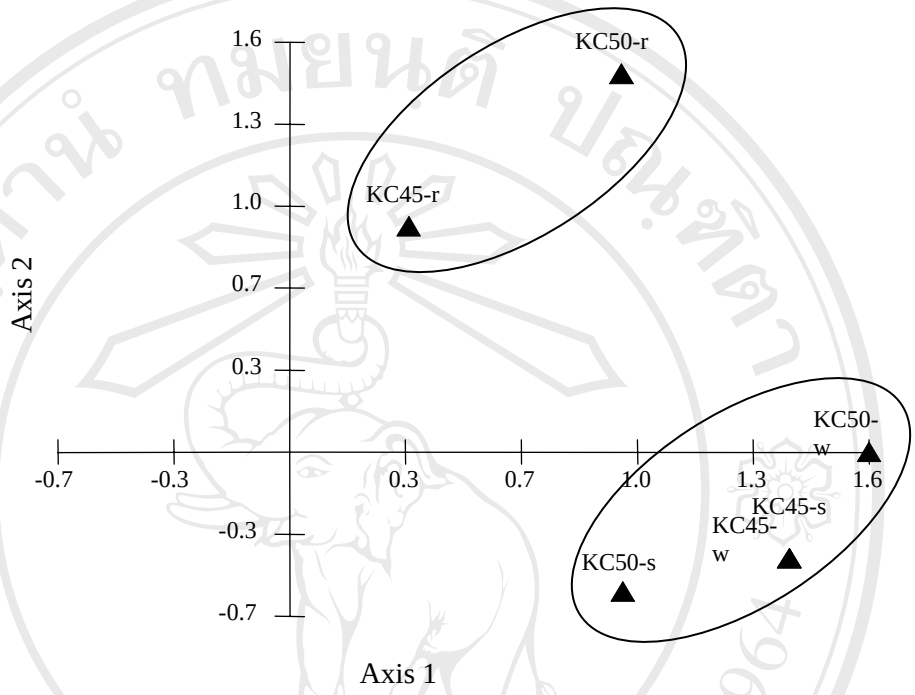

Figure 46. PCA ordination diagram of cyanobacterial DGGE profile distribution in Khaochaison Hot Spring

4.9 Phylogenetic analysis of the cyanobacterial 16S rDNA

All successfully sequenced 16S rRNA gene sequences were blasted against the complete non-redundant NCBI GenBank database, and those sequences found to share a high level of similarity were used to resolve alignment ambiguities and establish relationships for the sequences obtained in this study (Table 10).

Table 10. Identity of 37 sequences obtained from community DNA of thermophilic cyanobacterial mats

Clone [a]	Closest GenBank match		
	Identity	Accession Number	% Similarity
DGGE SK65-a	*Synechococcus* sp. C9	AF132773	95
DGGE SK55-a	*Oscillatoria terebriformis*	AF263343	96
DGGE SK60-b	*Cyanothece* sp. HPC-12	AY430161	90
DGGE SK50-a	*Oscillatoria terebriformis*	AF263343	96
DGGE SK45-a	*Phormidium mucicola*	AB003165	89
DGGE SK50-c	*Phormidium mucicola*	AB003165	88
DGGE SK50-b	*Oscillatoria terebriformis*	AF263343	95
DGGE SK55-c	*Oscillatoria* sp. NZ-TLS	AY426549	96
DGGE SK60-a	*Synechococcus* sp. C9	AF132773	95
DGGE SK65-b	*Synechococcus* sp. C9	AF132773	95
DGGE SK55-b	*Phormidium mucicola*	AB003165	89
DGGE PD65-a	*Synechococcus* sp. C9	AF132773	94
DGGE PD60-a	*Synechococcus* sp. C9	AF132773	94
DGGE PD50-a	Unknown Oscillatoriales	AF401748	89
DGGE PD45-a	*Oscillatoria terebriformis*	AF263343	96
DGGE PD45-b	*Oscillatoria* sp. WHS-4	AY426545	92
DGGE PD40-a	*Calothrix brevissima*	AB074504	92
DGGE TP60-a	*Pleurocapsa minor* PCC7327	Z82810	87
DGGE TP60-b	Unknown Oscillatoriales	AF401748	89
DGGE TP60-c	*Phormidium mucicola*	AB003165	89
DGGE TP55-b	*Oscillatoria terebriformis*	AF263343	96
DGGE TP55-d	*Leptolyngbya* sp. CNP1-B1-4	AY239603	93
DGGE TP50-b	*Synechococcus* sp. PCC7902	AF216946	90
DGGE TP55-c	Unknown Oscillatoriales	AF401748	89

Clone [a]	Closest GenBank match		
	Identity	Accession Number	% Similarity
DGGE TP50-a	*Phormidium mucicola*	AB003165	90
DGGE TP55-a	*Oscillatoria terebriformis*	AF263343	96
DGGE PR45-a	*Synechococcus* sp. C9	AF132773	98
DGGE PR45-b	*Chlorogloeopsis fritschii* PCC 6912	AB093489	95
DGGE PR45-c	*Phormidium mucicola*	AB003165	90
DGGE RS40-a	*Oscillatoria* sp. OH25	AF317508	99
DGGE RS40-b	Unknown Oscillatoriales IL-9.1	AF401743	95
DGGE RS45-a	*Synechococcus* sp. C9	AF132773	99
DGGE RS55-a	*Synechococcus* sp. C9	AF132773	99
DGGE RS55-b	*Mastigocladus* sp. Y-99-9	AY426547	95
DGGE RS55-c	*Oscillatoria* sp. OH25	AF317508	90
DGGE KC50-b	*Oscillatoria* sp. OH25	AF317508	99
DGGE KC50-c	*Oscillatoria amphigranulata* 19-2	AF317504	93
DGGE KC50-a	*Synechococcus* sp. C9	AF132773	99

[a] Letters denote mats from which each clone was obtained.

The overall phylogenetic tree generated for the 20 cyanobacterial samples isolated in this study (Table 11) and the related sequences from the NCBI database are shown in Figure 47. Cyanobacterial 16S rDNA gene trees were inferred by using Neighbor Joining, UPGMA and Maximum Parsimony methods. While there are topological differences among the three algorithms, they still clustered in the same clades. Members of the three genera (*Synechococcus*, *Phormidium*, and *Oscillatoria*) were indistinguishable using morphological analysis alone. Each group was separated into at least two distinct molecular lineages. The topology of these clades is consistent for all methods and is strongly supported by bootstrap value in all cases (Figure 47). The 16S rDNA sequence data used to build this phylogenic tree were based on 370-425 bp per sample, where an overall 98% sequence identity is generally considered to represent the same species, and <88% identity suggests separate genera (Hongmei *et al*., 2005; Stackebrandt and Goebel, 1994). These, of course, are arbitrary values based on well-known pathogenic bacteria.

Table 11 Twenty selected cyanobacterial enrichment cultures from all six hot springs

Cyanobacterial enrichment cultures	Morphotypes (main characteristics)
Chroococcidiopsis sp. PR45	Green colony,1.5-2.0 μm diameter
Chroococcidiopsis sp. PD60	Green colony,1.5-2.0 μm diameter
Chroococcidiopsis sp. KC45	Green colony,1.5-2.0 μm diameter
Chroococcidiopsis sp. RS40	Green colony,1.5-2.0 μm diameter
Cyanosarcina sp. SK40	Brown colony, 3.9-4μm diameter
Leptolyngbya sp. PR40	Green filament, 3.5 μm broad
Leptolyngbya sp. PD40	Green filament, 2x2-2.8μm, cross walls slightly constricted
Leptolyngbya sp. PD45	Green filament, straight, 2x 2μm
Leptolyngbya sp. KC45	Brown-red filament, curve filament (sometime), 2.5x3-3.2μm
Leptolyngbya sp. RS45	Green filament, 2x1.8-2μm
Leptolyngbya sp. SK40	Green filament, straight, 3-3.2x1μm
Oscillatoria sp. KC50	Green filament, cross walls slightly constricted, 1.2x2.8-3μm
Oscillatoria sp. TP65	Green filament, straight, 1 μm broad
Phormidium sp. PR40	Brown filament, cross walls slightly constricted, 1.2-1.3x2μm
Phormidium sp. PD45	Brown filament, cross walls slightly constricted, 2x2μm
Phormidium sp. RS40	Brown filament, cross walls slightly constricted, 1.5x1.8-2μm
Synechoccoccus sp. PD55	Unicellular, rod shape, 1.4-1.5μm broad
Synechoccoccus sp. SK40	Unicellular, rod shape, 1.2-1.5μm broad
Synechoccoccus sp. SK55	Unicellular, rod shape, 1.2-1.5μm broad
Synechoccoccus sp. TP65	Unicellular, rod shape, 1.2-1.5μm broad

Figure 47(a)

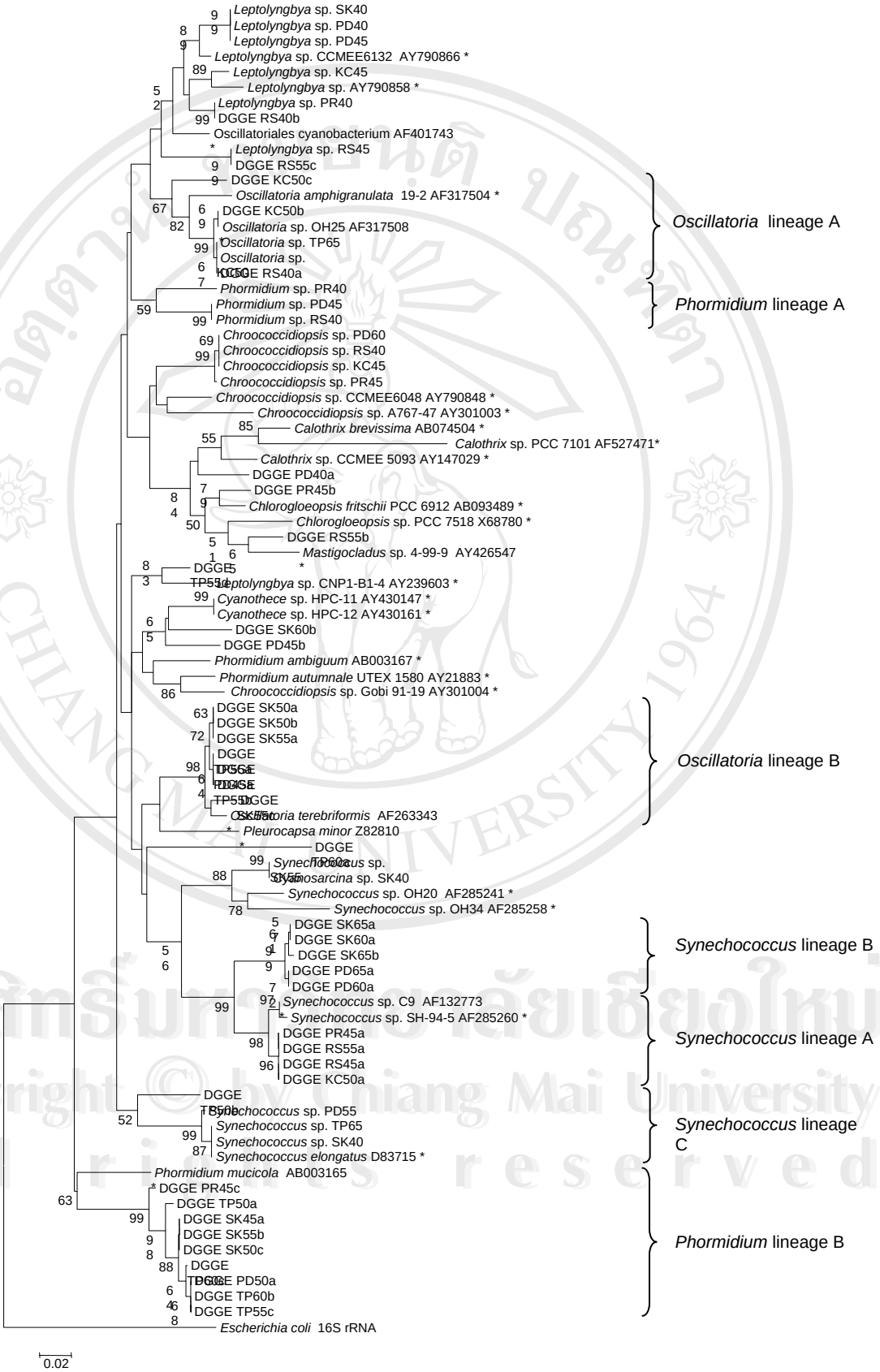

Figure 47(b)

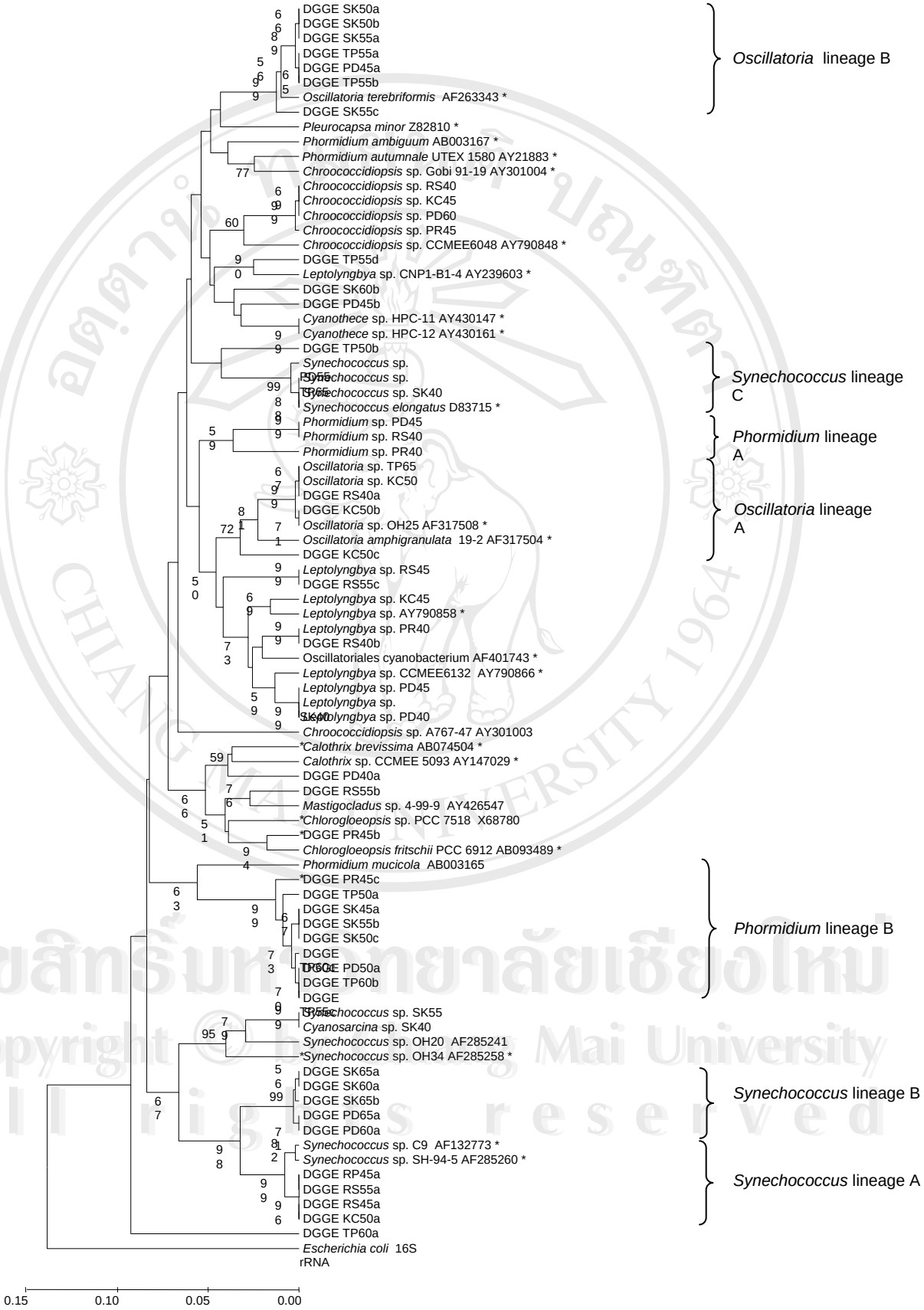

Figure 47(c)

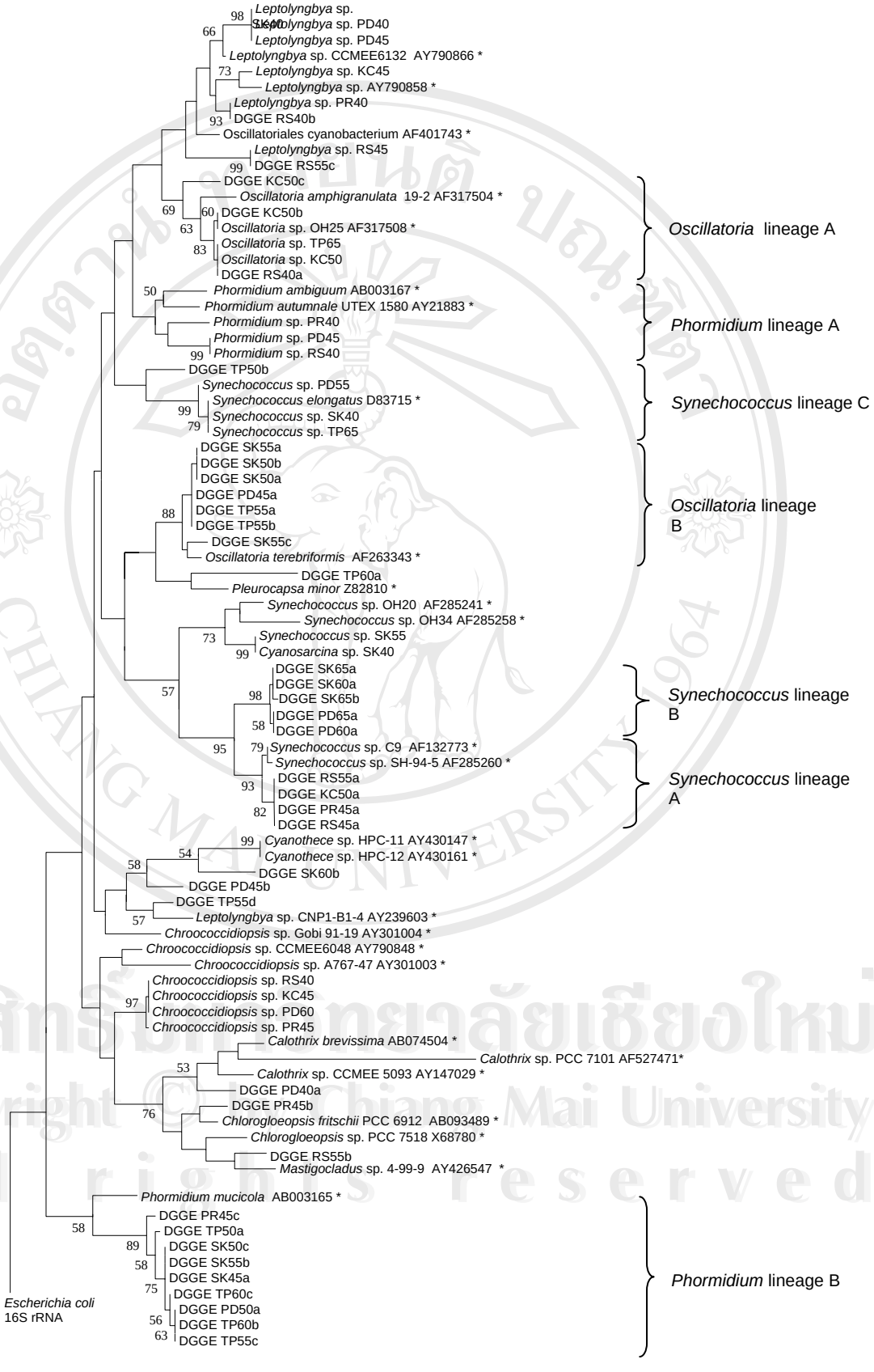

Figure 47. Phylogenetic relationships for the thermophilic cyanobacteria were constructed using partial 16S rRNA gene sequences, where evolutionary distances were determined using (a) Neighbor Joining analysis, (b) the UPGMA analysis and (c) Maximum Parsimony analysis with 1000 replicate bootstrap resampling to form the overall consensus tree. Sequence designations for DGGE samples are labeled by location, temperature (in 5°C intervals) and band position. The tree was rooted using *Escherichia coli* 16S rRNA sequence. Values at nodes indicate bootstrap percentages for the 1,000 replicates. Values at nodes indicate the bootstrap percentages where values less than 50% are not reported. Sequences marked with a (*) were obtained from NCBI.

The overall phylogenetic tree generated from these sequences suggested that several very similar morphotypes may be distinct species with similar morphology. Since it is not computationally feasible to check even a small fraction of all phylogenetic trees with over 30 lineages, the absolute relationships presented in Figure 47 were further examined to see if the molecular diversity was real or just a computational artifact. To verify the phylogenetic relationships for the three groups (*Synechococcus, Phormidium,* and *Oscillatoria*), the sequences from each group were reanalyzed individually with the addition of just a few morphologically distinct yet molecularly related species, as initially characterized in Figure 47, and the MP analysis was used to construct the consensus trees. The *Escherichia coli* 16S rDNA out group sequence which was used to root each tree.

The *Phormidium*-like cyanobacteria were found to contain two distinct molecular variants designated Lineages A & B as shown in Figure 48a. The five sequences in Lineage A, that were found in three Thailand springs (RS, PD, PR), share a 94.1% average identity to each other, whereas the nine sequences in Lineage B (excluding *Phormidium mucicola* which occurred exclusively in the north of Thailand) were much more closely related to each other with a 98.1% average identity. The phylogeny generated in Figure 48 upheld the overall phylogeny found in Figure 47 and clearly shows that the *Phormidium* in Lineage A are more closely related to the

morphologically distinct species *Leptolyngbya* sp. CNP1-B1-4 (89.1%) and *Synechococcus elongatus* D83715 (87.5%) than to the *Phormidium* in Lineage B (77.7%). However, none of these similarities are close enough to be meaningful.

Figure 48(a)

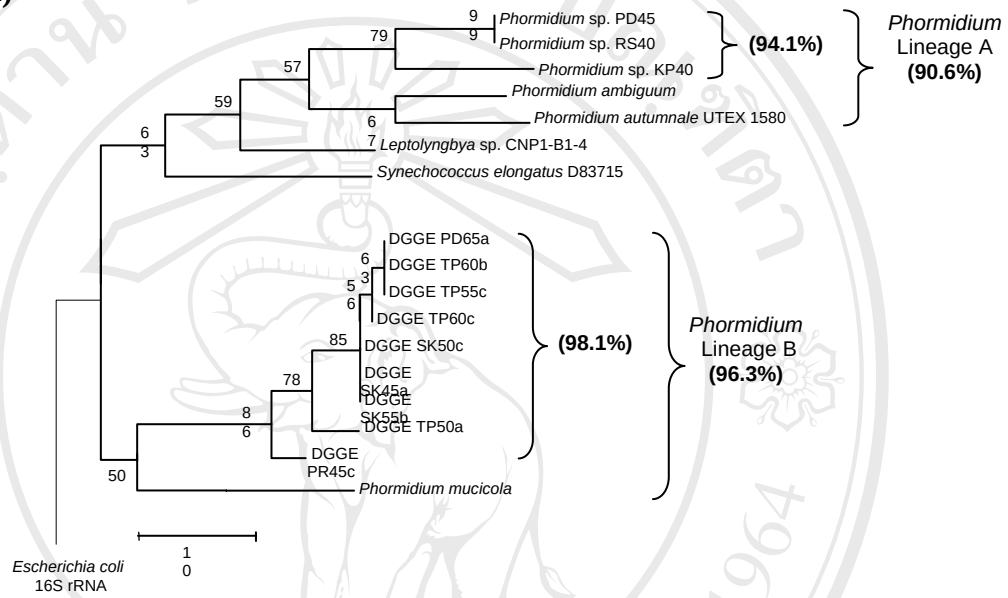

Figure 48(b)

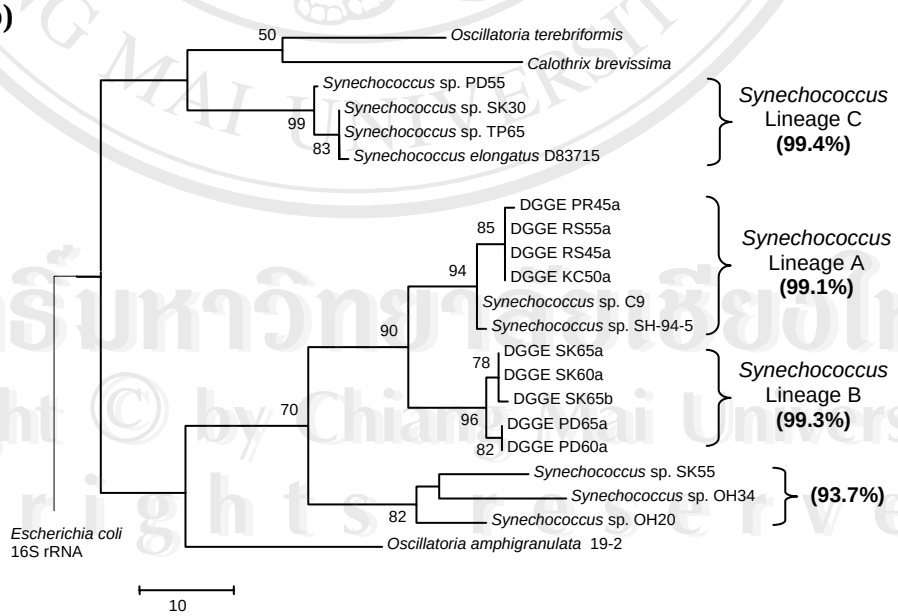

Figure 48(c)

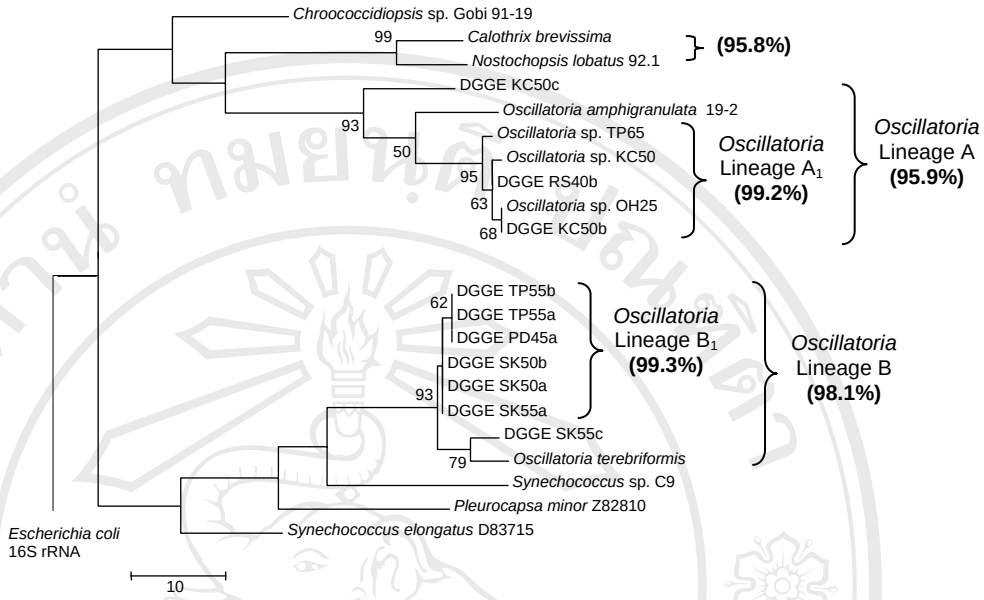

Figure 48. Phylogenetic relationships of the a) *Phormidium*-like, b) *Synechococcus*-like and c) *Oscillatoria*–like cyanobacteria were constructed on the basis of partial 16S rRNA gene sequences. Evolutionary distances were determined by the maximum parsimony analysis. The trees were rooted using the *Escherichia coli* 16Sr RNA sequence. Values at nodes indicate bootstrap percentages for 1,000 replicates. Values less than 50% are not reported. Percent values in parentheses indicate the average percent similarity within that group.

Several distinct lineages were found with distinct temperature and geographic distributions as shown in Figures 48b and 48c, respectively. For the *Synechococcus* groups, three distinct Lineages (A, B, and C) were found with over 99% average identity within each group. Lineage A was exclusively found in hot springs outside of the Chiang Mai region was also present at all temperature intervals lower than 60°C. Lineage B which was more closely related to Lineage A (94.2%) than to any other *Synechococcus* Lineage was found only in San Kamphaeng (SK) and Pong Dued (PD) Chiang Mai, and was found in all temperature ranges from 55°C and higher. All *Synechococcus* Lineages excluding lineage C were related at the 93% average identity level which places Lineages A and B at the same phylogenetic distance as

Synechococcus sp. SK5, OH34, and OH20. Lineage C, also found exclusively in the Chiang Mai region, shared a closer relationship to *Oscillatoria* cf. *terebriformis* (88.6%) and *Calothrix brevissima* (87.6%) than to any of the other *Synechococcus* Lineages (81.9%). Although *Synechococcus* Lineage C is morphologically similar to the other *Synechococcus* species groups, it is clearly distinct and more closely related to other morphologically distinct species.

However, none of these distant similarities are meaningful, and reflect the shortage of sequences in the database. The *Oscillatoria* group was found to break into two distinct lineages each of which was more closely related to morphologically distinct cyanobacteria than to the other lineage. For these two lineages, subgroups A_1 and B_1 were found to be related at the 99% identity level within each subgroup and between the two subgroups there was only a 79.5% average identity level. Both subgroups were only found at temperatures lower than 60°C, where *Oscillatoria* subgroup A_1 was found to have no geographical barriers and *Oscillatoria* subgroup B_1 was found to be geographically limited to the northern region.